1521-009X/50/4/386–400$35.00
DRUG METABOLISM AND DISPOSITION
dx.doi.org/10.1124/dmd.121.000711
Drug Metab Dispos 50:386–400, April 2022

Prediction of Maternal and Fetoplacental Concentrations of Cefazolin, Cefuroxime, and Amoxicillin during Pregnancy Using Bottom-Up Physiologically Based Pharmacokinetic Models[S]

Khaled Abduljalil, Jia Ning, Amita Pansari, Xian Pan, and Masoud Jamei

Certara UK Limited, Simcyp Division, Sheffield, United Kingdom

Received October 5, 2021; accepted January 4, 2022

ABSTRACT

Concerns over maternal and fetal drug exposures highlight the need for a better understanding of drug distribution into the fetus through the placental barrier. This study aimed to predict maternal and fetal drug disposition using physiologically based pharmacokinetic (PBPK) modeling. The detailed maternal-placental-fetal PBPK model within the Simcyp Simulator V20 was used to predict the maternal and fetoplacental exposure of cefazolin, cefuroxime, and amoxicillin during pregnancy and at delivery. The mechanistic dynamic model includes physiologic changes of the maternal, fetal, and placental parameters over the course of pregnancy. Placental kinetics were parametrized using permeability parameters determined from the physicochemical properties of these compounds. Then, the PBPK predictions were compared with the observed data. Fully bottom-up fetoplacental PBPK models were developed for cefuroxime, cefazolin, and amoxicillin without any parameter fitting. Predictions in nonpregnant subjects and in pregnant subjects fall within 2-fold of the observed values. Predictions matched observed pharmacokinetic data reported in nine maternal (five fetoplacental) studies for cefuroxime, 10 maternal (five fetoplacental) studies for cefazolin, and six maternal (two fetoplacental) studies for amoxicillin. Integration of the fetal and maternal system parameters within PBPK models, together with compound-related parameters used to calculate placental permeability, facilitates and extends the applications of the maternal-placental-fetal PBPK model. The developed model can also be used for designing clinical trials and prospectively used for maternal-fetal risk assessment after maternally administered drugs or unintended exposure to environmental toxicants.

SIGNIFICANCE STATEMENT

This study investigates the performance of an integrated maternal-placental-fetal PBPK model to predict maternal and fetal tissue exposure of renally eliminated antibiotics that cross the placenta through a passive diffusion mechanism. The transplacental permeability clearance was predicted from the drug physicochemical properties. Results demonstrate that the PBPK approach can facilitate the prediction of maternal and fetal drug exposure simultaneously at any gestational age to support its use in the maternal-fetal exposure assessments.

Introduction

Various physiologic and biochemical changes that occur during pregnancy can affect pharmacokinetics (PK) of administered compounds (Abduljalil et al., 2020c). Currently, most drugs carry warnings or contraindications for their use during pregnancy. Obstetricians frequently prescribe drugs for indications other than those on the product label, and this unlicensed or off-labeled use may be necessary if the clinical need cannot be met by licensed medicines. Such use should be supported by appropriate evidence that balances benefits and risks associated with maternal-fetal drug exposure (Rayburn and Farmer, 1997).

Approximately one in four women will be prescribed an antibiotic during pregnancy, accounting for nearly 80% of prescription medications in pregnant women (Bookstaver et al., 2015). Although many antibiotics have been reported to be safe, such as penicillins and cephalosporines, there are some antibiotics that should be avoided entirely during pregnancy (Muanda et al., 2017). Different antibiotics can cross the placenta and reach the fetus, achieving fetal exposures comparable to the mother (Pacifici, 2006; Viel-Theriault et al., 2019).

Traditionally, the extent of the drug passage through the placenta is assessed by comparing the drug concentration in the umbilical cord at birth to the maternal drug concentration; however, such measurements are still challenging because only one sample can be obtained per subject within a short time frame and the sampling time is relative to the last maternal dose taken. Sampling placenta, fetal organs, or systemic circulation during pregnancy for PK evaluation can be challenging and unethical. Experimentally, fetal drug exposure remains difficult to quantify, as the fetus and placenta are not readily accessible for sampling until delivery. Various animal models have been used to study placental drug transfer, but data are of poor translational value due to interspecies variability in placental types and structures (Schmidt et al., 2015; Bouazza et al., 2019). On the other hand, an ex vivo human placenta

No funding was received for the preparation of this study.

All authors are full-time employees of Certara UK Limited, Simcyp Division. The activities of Certara are supported by a consortium of pharmaceutical companies. The Simcyp Simulator is freely available, after completion of the training workshop, to approved members of academic institutions and other not-for-profit organizations for research and teaching purposes.

dx.doi.org/10.1124/dmd.121.000711.

[S] This article has supplemental material available at dmd.aspetjournals.org.

ABBREVIATIONS: CL, clearance; GFR, glomerular filtration rate; GW, gestational week; HBD, hydrogen bond doner; Kp, tissue-to-plasma partition ratio; MechKiM, mechanistic kidney model; MRP4, multidrug resistance protein 4; OAT, organic anion transporter; PBPK, physiologically based pharmacokinetics; PK, pharmacokinetics; PSA, polar surface area.

perfusion experiment that uses a single placental cotyledon has shown to be a useful model for studying the transplacental passage of various drugs (Bouazza et al., 2019).

Pregnancy physiologically based pharmacokinetic (PBPK) models that incorporate adequately detailed maternal and fetal physiologic parameters are suitable tools that can facilitate the assessment of fetal exposure when placental kinetics are also integrated in the model (De Sousa Mendes et al., 2017; Schalkwijk et al., 2018; Bouazza et al., 2019). Applications of PBPK models to describe fetal exposure are increasing and have been published for many drugs, including emtricitabine, tenofovir, nevirapine, midazolam, theophylline, darunavir, dolutegravir, zidovudine, and acetaminophen (see Abduljalil and Badhan, 2020). In most of these examples, transplacental transfer parameters were estimated from the ex vivo human placenta perfusion experiments and were then integrated within the pregnancy PBPK models using appropriate scaling from a single cotyledon to the whole placenta. Those models included at least one compartment to reflect the anatomy of the fetus. Although the majority of drugs have not been studied using the placental ex vivo perfusion, it is of interest to develop a predictive algorithm to allow prediction of placental pharmacokinetic parameters, mainly passive diffusion across both sides of the placenta.

The aim of this study is to use the multicompartmental fetoplacental PBPK model within the Simcyp Simulator V20 to assess the possibility of predicting the fetal exposure using physicochemical properties of three mainly renally cleared antibiotics: cefuroxime, cefazolin, and amoxicillin. These compounds were chosen due to observed data availability. PBPK predictions at different time points during gestation were compared with the clinically observed data.

Materials and Methods

General Settings

The pregnancy model within the Simcyp Simulator V20 was used for all predictions in the current study. The pregnancy model accounts for physiologic parameters, interindividual variability, and their changes during the whole gestational period. Growth and decline of the physiologic parameters during pregnancy are incorporated in the model as continuous functions to allow predictions at different gestational ages. The model considers the continuous change of all physiologic and biologic parameters simultaneously over time and within each subject to account for any time-varying covariates.

The model structure includes a multicompartment fetal PBPK model coupled with the maternal PBPK model via a permeability-limited placenta model. It includes previously reported physiologic changes that occur during pregnancy, including maternal (Abduljalil et al., 2012) and fetal physiology (Abduljalil et al., 2018; 2019; 2020a; 2021). A basic perfusion-limited version of a PBPK model consisting of 14 compartments representing various fetal tissues was linked to the Simcyp maternal full-PBPK model via the placenta, which in turn was represented by three compartments (Fig. 1). Amniotic fluid is modeled using a single compartment. Previously published nonlinear differential equations describing the structure of the model, with its code for the fetus, placenta, and amniotic fluid, were used for the model building (Zhang et al., 2017). These equations are based on the mass conservation law describing the changes in drug concentration over time after maternal drug administration. In the current study, however, the model has been further expanded to include eight additional fetal tissues: spleen, pancreas, muscle, bone, adipose, heart, lung, and skin. Physiologic parameters required for fetal PBPK model specifications and their changes during pregnancy were taken from a recent series of published meta-analyses of physiologic, biologic, and anatomic measurements on total body weight, height, surface area, gross body composition (Abduljalil et al., 2018), organ volumes and compositions (Abduljalil et al., 2019), blood and binding components (Abduljalil et al., 2020a), and organ blood flows (Abduljalil et al., 2021). Equations describing longitudinal changes in fetal physiologic parameter values from these references were incorporated into the fetal PBPK model and coupled to the maternal PBPK model within the Simulator.

The amniotic fluid is mainly composed of water, and its volume increases with pregnancy progression according to our previously published data (Abduljalil et al., 2012). The model assumes that the administered drug reaches the amniotic fluid via fetal renal clearance and leaves the amniotic fluid back into the fetal circulation via fetal swallowing activity and intramembranous diffusion.

Model Building

For all evaluated compounds, distribution was defined using a full PBPK distribution model that accounts for different tissue volumes and flow rates. Drug tissue-to-plasma partition ratios (Kps) were predicted within the Simulator for these compounds using the Rodgers and Rowland method (Rodgers and Rowland, 2006) (see below for more detail). Elimination of the drugs was described using the mechanistic kidney model (MechKiM) to account for renal transporter kinetics (Neuhoff et al., 2013). No fetal hepatic clearance was assumed for these compounds.

Before predicting the drug kinetics during pregnancy, all compound PBPK models were first built and verified for their performances in the nonpregnant population as described earlier (Abduljalil et al., 2020c). Once the PBPK model adequately predicted the drug kinetics in nonpregnant subjects, the settings were retained to predict the drug kinetics in pregnant women at different gestational weeks (GWs). Predictions, in all cases, were performed via matched virtual population demographics, and trial simulation settings/designs to the original studies. Predicted PK profiles and PK parameters were compared with different sets of clinical observations available in the literature. Default demographics and age range were used when corresponding data were not provided in the original paper.

No data from ex vivo human placenta perfusion experiments were available for the three compounds of interest here; therefore, to parametrize the full fetoplacental model, the compound hydrogen bond doner (HBD) and polar surface area (PSA) are used to predict the transplacental passive permeability of cefuroxime using eq. 1 (Yang et al., 2007):

$$P_{eff}(10^{-4} cm/s) = 10\ \hat{}\ (1.454 - 0.011\ PSA - 0.278\ HBD) \quad (1),$$

where *PSA* is polar surface area and *HBD* is the hydrogen bond donor of the compound. Then, the placenta diffusion clearance CL_{PD} was calculated as follows (eq. 2):

$$CL_{PD}(L/h/mL\ of\ Placenta) = P_{eff}\ \left(\frac{3.6\ PVSA}{Vol.Placenta}\right) \quad (2),$$

where *PVSA* is the placenta villus surface area at term ($PVSA = 11\ m^2$) (Boyd, 1984; Teasdale and Jean-Jacques, 1985; Mayhew, 2001), *Vol.Placenta* is the placental volume at term in milliliters (665 ml), and 3.6 is a unit conversion scalar. The placental permeability clearance input in the model is in ml/min/ml of placental volume unit. This approach is useful to allow scaling the permeability to early gestational weeks based on the placental volume.

At term, the fetus swallows on average 400 ml of amniotic fluid per day (Blackburn, 2007). Therefore, this value was used to describe the swallowing activity clearance in the model (i.e., $CL_{swallowing}$ (l/h/kg fetal weight) = 0.00476l/h/kg fetal weight). Additionally, the intramembranous pathway transfers about 200–500 ml per day of fluid and solutes from the amniotic cavity to the fetal circulation across the amniotic membranes (see Underwood et al., 2005). This flow has been calculated using 350 ml per day and normalized to 3.5 kg of fetal body weight at term (i.e., $CL_{intramembranous}$ = 0.00417 l/h/kg). The combined fetal $CL_{Swallowing}$ and $CL_{intramembranous}$ ($CL_{Swallowing}$ + $CL_{intramembranous}$ = 0.00893 l/h/kg) was considered as a system parameter and incorporated into the model for all compounds. The $CL_{intramembranous}$ is assumed to be a bidirectional flow and added to the calculated fetal renal clearance (*fetal* CL_R), as they both use the same deriving concentration (i.e., fetal systemic venous concentration) (see supplemental material in Zhang and Unadkat, 2017). The *fetal* CL_R itself was calculated with reference to an adult glomerular filtration rate (GFR) of 121 ml/min (Rhodin et al., 2009) according to the following equation (eq. 3) and assuming a fetal body weight of 3.5 kg at term:

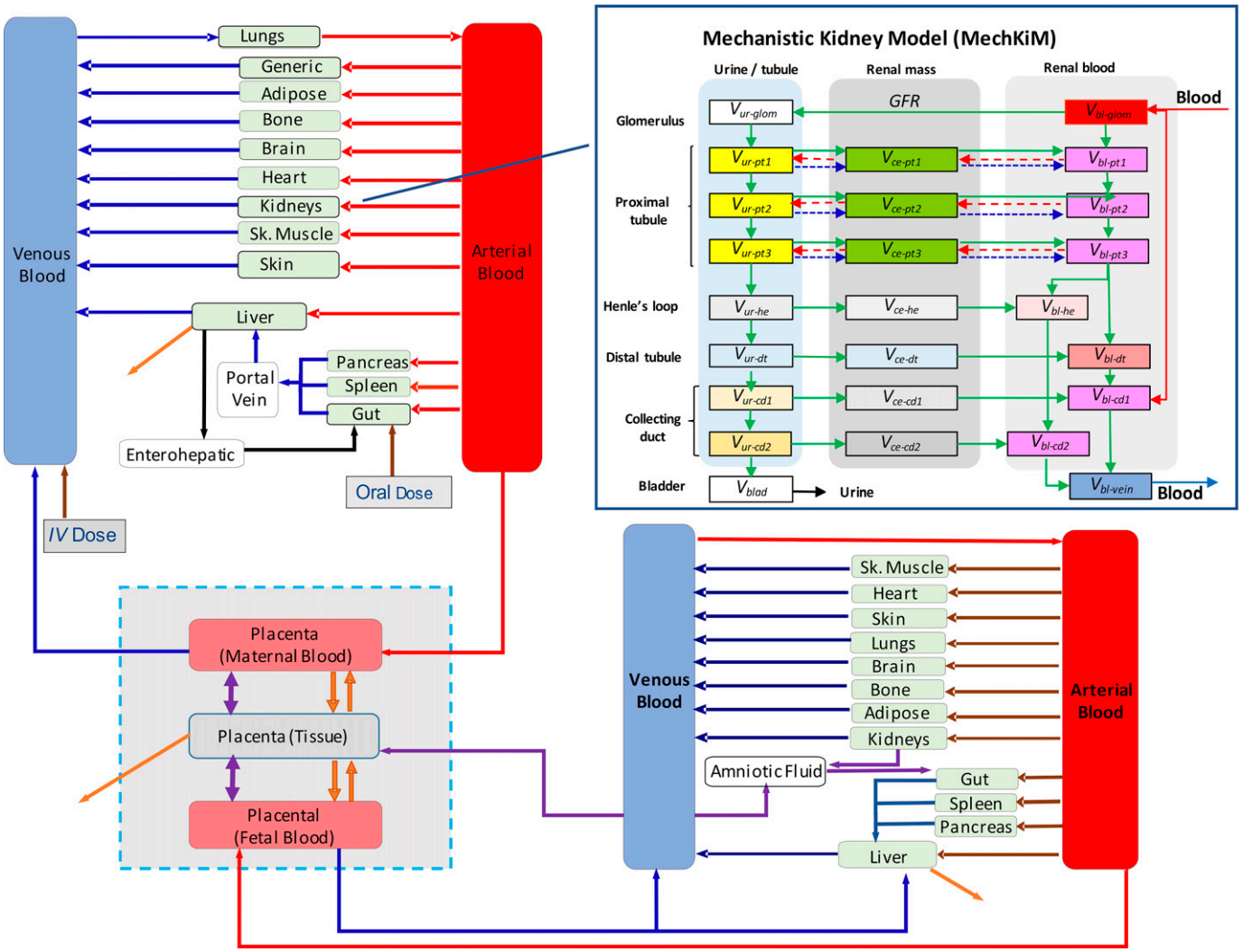

Fig. 1. Structure of the full maternal-placental-fetal model within the Simcyp Simulator V20 coupled with the MechKiM model. Note: For the MechKiM model, both renal blood flow and GFR are gestational age-dependent; hence, the flows between kidney compartments are gestational age-dependent (solid black arrows). Broken arrows represent directions of efflux and uptake transporters.

$$fetal\ CL_R(L/h/kg) = \left(\frac{Adult\ CL_R\ (L/h)}{Fetal\ Bodyweight(Kg)}\right) \times \left(\frac{Urine\ Flow\ (\mathrm{mL/min})}{Adult\ GFR\ (\mathrm{mL/min})}\right) \quad (3)$$

The fetal urine flow rate at term was about 1.39 ml/min (weighted mean of observations from Lee et al., 2007; Touboul et al., 2008; and Maged et al., 2014).

Cefuroxime

Cefuroxime is a second-generation cephalosporin antibiotic for treatment of several infections during pregnancy (Alrammaal et al., 2019). Cefuroxime is primarily cleared by the kidney as unchanged drug (about 97.3% of the administered dose), and its renal clearance correlates well with urine flow and creatinine clearance in normal as well as in impaired renal function (van Dalen et al., 1979). Both glomerular filtration and tubular excretion are involved with about 40%–49% of the renal excretion of cefuroxime via tubular excretion (Gower and Dash, 1977; Verhagen et al., 1994). Different studies investigated cefuroxime kinetics during pregnancy and its passage across the placenta during pregnancy (Bousfield et al., 1981; Craft et al., 1981; Philipson and Stiernstedt, 1982; Roumen et al., 1990; De Leeuw et al., 1993; Holt et al., 1993; 1994).

Model Building

A PBPK model for cefuroxime for the nonpregnant population has already been published and verified after ascending intravenous (i.v.) doses in healthy male subjects (Hsu et al., 2014). In that model, due to lack of data, cefuroxime was assumed to reach the kidney cells through an active process and hence was described using a generic basolateral transporter. Once the drug entered the renal cells, it was pumped out of the cells into the urine via the multidrug resistance protein 4 (MRP4) transporter (see Hsu et al., 2014). The original model inputs were used in the current work and were expanded to intramuscular (i.m.) administration with a first-order absorption rate constant of 1.2 (30% CV) and complete absorption (fraction absorbed, fa =1.0 with associated10% CV), to describe observed data after a 750-mg intramuscular dose (O'Callaghan and Harding, 1977). The list of the model inputs is given in Supplemental Table 1. Predicted exposure in the nonpregnant population was compared with the observed data.

To extend the nonpregnant cefuroxime PBPK model to predict kinetics during pregnancy, the pregnancy population was used and the permeability-limited placenta model, together with the full PBPK fetal model, was selected. Calculating cefuroxime placental permeability from HBD and PSA and scaling it up to the placenta (eq. 1 and 2) resulted in CL_{PD} of 0.0016 l/h/ml of placenta (at term). This value was used as diffusion clearances at both sides of the placenta. Based on adult cefuroxime CL_R of 3.5 l/h (Hsu et al., 2014), the resulted fetal cefuroxime CL_R according to eq. 3 was 0.0390 l/h/kg. As mentioned earlier, the

$CL_{intramembranous}$ is a bidirectional flow , hence, the combined fetal CL_R + $CL_{intramembranous}$ = 0.043 l/h/kg was incorporated in the model before executing the simulations. Cefuroxime is known for its renal toxicity in human and mice with reported data indicated that the drug reached similar concentrations in kidney as in the systemic circulation (Hvidberg et al., 2000). Although the drug concentration in the maternal kidney is described mechanistically using the MechKiM model, the fetal Kp for the kidney was set to 1. All other fetal tissue-to-plasma partition coefficients (Kps) were predicted within the Simulator using the Rodgers and Rowland method (Rodgers and Rowland, 2006) without any adjustment to the calculated tissue Kps.

Predicted exposure in the pregnant population was compared with the observed data. The following virtual trial designs were used to predict cefuroxime in pregnant subjects after maternal administration:

Trial Design P1. Single intravenous bolus of 750 mg cefuroxime given over a period of 1 minute (Philipson and Stiernstedt, 1982); 20 trials of seven pregnant women at 11–35 GWs and aged 20–45 years (default Simulator settings).

Trial Design P2. Single intravenous bolus of 750 mg cefuroxime given over a period of 1 minute (Philipson and Stiernstedt, 1982); 20 trials of seven pregnant women at 37–42 GWs and aged 20–45 years.

Trial Design P3. Single intravenous bolus of 750 mg cefuroxime given over a period of 3 minutes (Holt et al., 1994); 20 trials of 26 pregnant women at 35–40 GWs and aged 20–45 years.

Trial Design P4. Single intravenous bolus of 1500 mg cefuroxime given over a period of 3 minutes (Holt et al., 1994); 20 trials of 13 pregnant women at 38–40 GWs and aged 20–45 years.

Trial Design P5. Single intravenous bolus of 750 mg cefuroxime given over a period of 3 minutes (Holt et al., 1993); 20 trials of 78 pregnant women at 38–40 GWs and aged 20–45 years.

Trial Design P6. Single intravenous bolus of 750 mg cefuroxime given over a period of 1 minute (Bousfield et al., 1981); 20 trials of 10 pregnant women at term (40 GWs) and aged 18–32 years.

Trial Design P7. An intravenous bolus of 750 mg cefuroxime given over a period of 1 minute followed by a similar dose after 4 hours (Bousfield et al., 1981); 20 trials of 10 pregnant women at term (40 GWs) and aged 18–32 years.

Trial Design P8. Single intramuscular injection of 750 mg cefuroxime (Craft et al., 1981); 20 trials of 22 pregnant women at term (40 GWs) and aged 18–45 years.

Trial Design P9. Multiple intravenous infusions of 1500 mg cefuroxime given over a period of 10 minutes every 8 hours (Roumen et al., 1990; De Leeuw et al., 1993); 20 trials of 10 pregnant women at 27–35 GWs and aged 23–45 years.

Trial Design P10. Single intravenous bolus of 750 mg cefuroxime given over a period of 1 minute (Takase et al., 1979); 10 trials of 29 pregnant Japanese women at term (40 GWs) and aged 20–45 years (use of sim-pregnancy population file with Japanese females' body weight/height and kidney parameters).

Cefazolin

Cefazolin is commonly prescribed as a prophylactic antimicrobial agent for a variety of surgical interventions, including cesarean section. The drug is administered via intravenous or intramuscular routes. Different clinical studies have evaluated the pharmacokinetics of cefazolin during late pregnancy and have reported the concentrations in maternal circulation, the umbilical cord, and amniotic fluid (Bernard et al., 1977; Philipson et al., 1987; Brown et al., 1990; Fiore Mitchell et al., 2001; Allegaert et al., 2009; Elkomy et al., 2014; van Hasselt et al., 2014; Grupper et al., 2017; Kram et al., 2017).

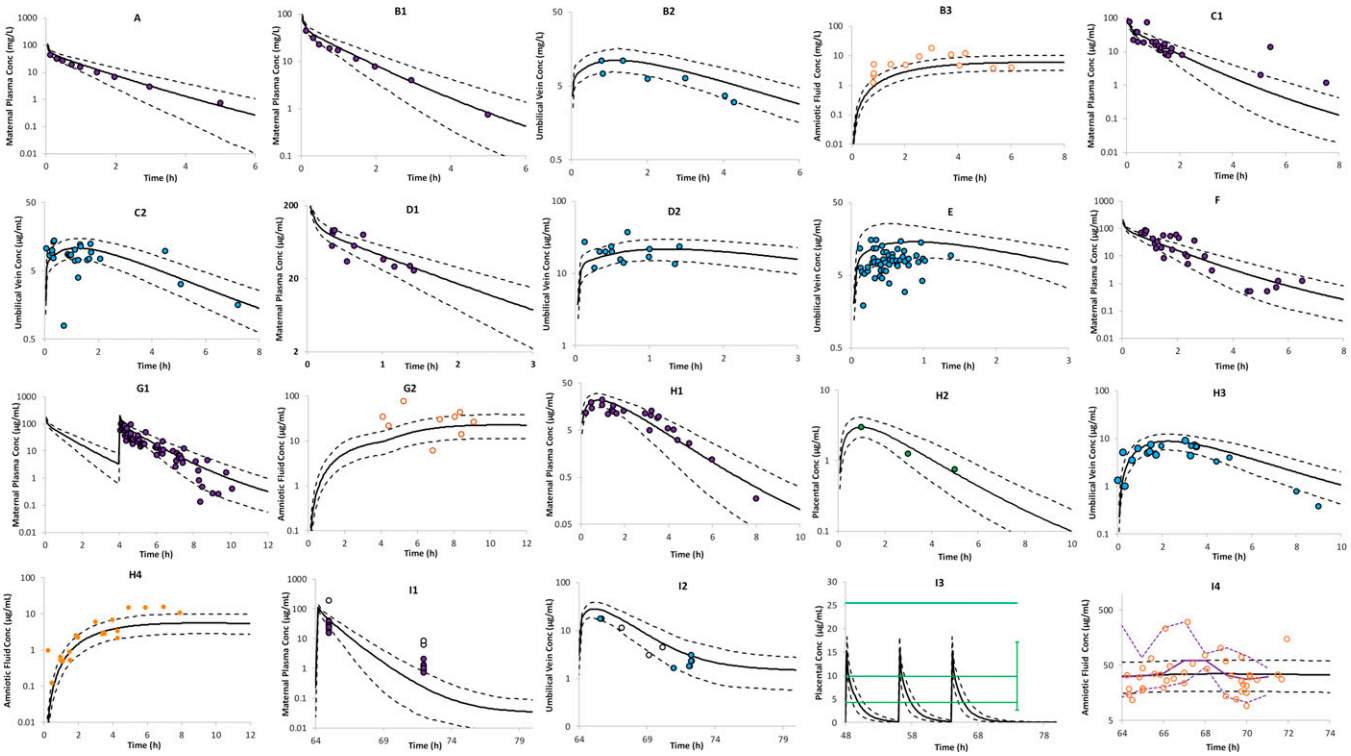

Fig. 2. (A) PBPK predicted (lines) vs. observed (circles) cefuroxime concentration profiles in pregnant women after intravenous (Plots A–G2) and intramuscular (Plots H1–H4) doses. Plot A: 750 mg over 1 minute at 11–35 GWs (Philipson and Stiernstedt, 1982); Plots B1 and B3: 750 mg over 1 minute at 37–42 GWs (Philipson and Stiernstedt, 1982); Plots C1 and C2: 750 mg over 3 minutes at 35–40 GWs (Holt et al., 1994); Plots D1 and D2: 1500 mg over 3 minutes at 38–40 GWs (Holt et al., 1994); Plot E: 750 mg over 3 minutes at 38–40 GWs (Holt et al., 1993); Plot F: 1500 mg over 1 minute at term (Bousfield et al., 1981); Plots G1 and G2: two A doses of 1500 mg cefuroxime over 1 minute at term repeated after 4 hours (Bousfield et al., 1981); Plots H1–H4: 750 mg i.m. at term (Craft et al., 1981); and Plots I1–I4: 1500 mg i.v. every 8 hours (Roumen et al., 1990; De Leeuw et al., 1993) with filled circles in I1 and I2 from Roumen et al. (1990). Horizontal lines in I3 represent minimum, geometric mean, and maximum values from nine placental homogenate samples (sampling times were not available), error bar represents standard deviation, and profiles in I4 represent reported minimum, median, and maximum values from 81 amniotic fluid samples (De Leeuw et al., 1993). Observed concentrations are shown as open circles (maternal), orange circles (umbilical vein plasma), and blue circles (amniotic fluid). Bold continuous lines are the predicted means. Broken lines are the 5th and 95th percentiles. See *Materials and Methods* for trial settings. (B) PBPK predicted vs. observed (circles) maternal, placental, amniotic, and fetal cefuroxime concentration after administration of a single i.v. bolus of 750 mg cefuroxime (Takase et al., 1979) to pregnant women at term (40 GWs). Bold continuous lines are the predicted means. Broken lines are the 5th and 95th percentiles. See *Materials and Methods* for trial settings.

Model Building

A PBPK model for cefazolin was built using published physicochemical properties and experimental data as well as predictive algorithms within the Simulator. In brief, the distribution was described using the full PBPK distribution model with the tissue-to-plasma partition coefficients being predicted using the Rodgers and Rowland method (Rodgers and Rowland, 2006) with a global Kp scalar of 0.7 to match observed data after a 1000-mg intravenous dose (Rattie and Ravin, 1975). Cefazolin elimination was described using the MechKim and additional nonspecific hepatic metabolism. The elimination through the kidney was described using permeability clearance on both sides of the renal cells and active transporters at the proximal tubules using the basolateral organic anion transporters OAT1 and OAT3 uptake transporters (Mathialagan et al., 2017) as well as the apical MRP4 efflux transporter (Ci et al., 2007). The model then extended to the intramuscular route using a reported intramuscular absorption rate constant of 1.0 l/h (Scheld et al., 1981). See Supplemental Table 1 for the list of the model input. Predicted exposure in the nonpregnant and pregnant populations was compared with the observed data.

To extend the model to predict cefazolin disposition during pregnancy, the pregnancy population was used with the permeability-limited placenta model and the full PBPK fetal model being selected. A recent study reported that the renal OAT3 activity increased by approximately 2.2-, 1.7-, and 1.3-fold during the first, second, and third trimesters, respectively (Peng et al., 2021). These data were described using the following function:

$$\text{Renal OAT3}_{pregnancy} = 1 * (1 + 0.195 * \text{GW} - 0.0093 * \text{GW}^2 + 0.0001154\, GW^3) \quad (4),$$

where GW is the gestational week. This equation was added to the model to predict renal clearance during pregnancy at any gestational week. Although no informative data could be found to describe the longitudinal changes in renal OAT1 and MRP4 transporters during pregnancy, the nonpregnant values were retained for these two transporters.

Few reports have documented rapid placental passage of intravenously administered cefazolin to umbilical cord blood and amniotic fluid (Philipson et al., 1987; Allegaert et al., 2009; Elkomy et al., 2014; van Hasselt et al., 2014). These studies indicated that cefazolin can readily cross the placenta; however, no data from an ex vivo human placenta perfusion experiment were available. For parametrizing the full fetoplacental model, the compound HBD and PSA were used to predict the transplacental passive permeability of cefazolin as explained earlier for cefuroxime. This resulted in a placental CL_{PD} clearance value of 0.0012 l/h/ml of placenta. This value was then applied to both the maternal-faced (CL_{PDM}) and fetal-faced (CL_{PDF}) clearances of the placenta.

The fetal cefazolin CL_R was calculated from the adult cefazolin CL_R, as described earlier under the cefuroxime example, resulted in a fetal cefazolin CL_R estimate of 0.0130 l/h/kg fetal weight at term. Then the combined fetal CL_R + $CL_{intramembranous}$ = 0.0172 l/h/kg was incorporated into the model. Fetal tissue-to-plasma partition coefficients (Kps) were predicted within the Simulator using the Rodgers and Rowland method (Rodgers and Rowland, 2006) without any adjustment to the calculated tissue Kps. Performance of the developed model was verified against different clinical studies.

The following virtual trial designs were set for model building and prediction in pregnant subjects after the cefazolin administration:

Trial Design P1. Single intravenous dose of 2000 mg cefazolin infused over 10 minutes (van Hasselt et al., 2014); 20 trials of 20 pregnant women at 17–27 GWs and aged 18–45 years.

Trial Design P2. Single intravenous dose of 2000 mg cefazolin infused over 10 minutes (van Hasselt et al., 2014); 20 trials of 20 pregnant women at 28–34 GWs and aged 18–45 years.

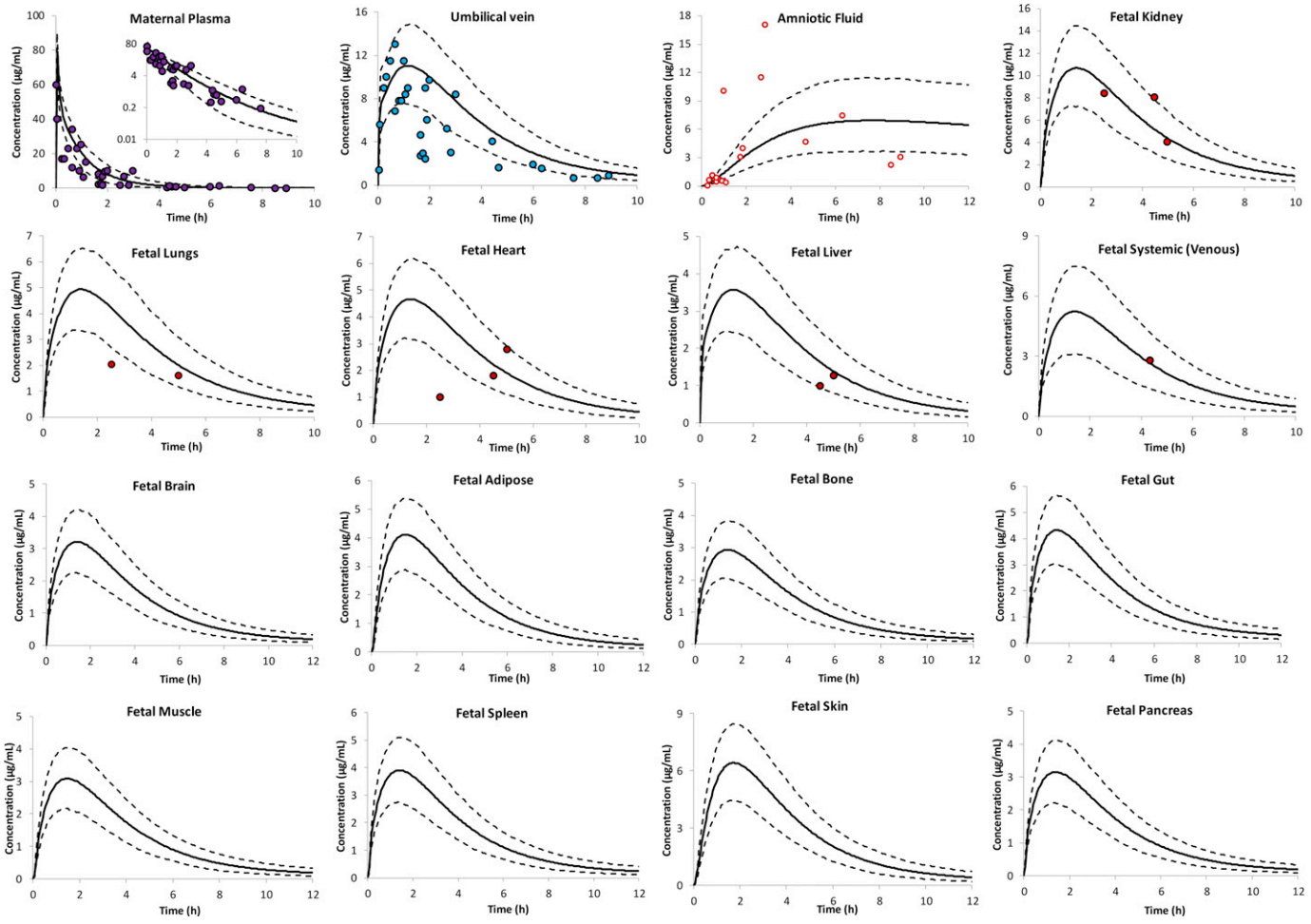

Fig. 2 (CONT.)

TABLE 1

Predicted vs. observed PK parameters of cefuroxime in nonpregnant subjects and during pregnancy after i.v. or i.m. administration
Results are expressed as mean (S.D.); *mean (range).

	Study design; Population *n* (%F)	GWs	CL (l/h)			AUC (mg h/l)			Half-Life (h)		
			Obs	Pred	Ratio	Obs	Pred	Ratio	Obs	Pred	Ratio
Nonpregnant	Single 0.75-g i.v. infusion; 10 (50%) (Garton et al., 1997)	NA	10.0	11.0 (3.2)	1.13	77.0 (10)	73.0 (22)	0.95	NA	0.86 (0.24)	NA
	Single 1.5-g i.v. infusion; 10 (50%) (Garton et al., 1997)	NA	11.0	11.0 (3.2)	1.00	137 (20)	147 (44)	1.07	NA	0.86 (0.24)	NA
	Single 0.667-g i.v. bolus; 20 (50%) (Thonnings et al., 2020)	NA	16.0 (2.1)	11.0 (3.1)	0.69	41.7	67.0 (19)	1.63	NA	0.90 (0.25)	NA
	Single 1.375-g i.v. bolus; 20 (50%) (Thonnings et al., 2020)	NA	16.0 (2.1)	11.0 (3.1)	0.69	85.9	137 (39)	1.59	NA	0.90 (0.25)	NA
	Single 0.5-g i.v. bolus; 6 (0%) (Gower and Dash, 1977)	NA	9.4 (2.5)	11.1 (3.3)	1.18	53.1 (18.1)	49.3 (15)	0.93	1.14 (0.26)	0.95 (0.24)	0.83
	Single 0.75-g i.v. bolus; 6 (0%) (Gower and Dash, 1977)	NA	10.1 (1.5)	11.1 (3.3)	1.10	74.0 (13.8)	73.9 (22.4)	1.00	1.10 (0.27)	0.95 (0.24)	0.86
	Single 0.25-g i.v. bolus; 3 (0%) (Foord, 1976)	NA	7.67	11.6 (3.4)	1.51	32.6 (1.1)	23.6 (7.6)	0.72	1.0 (0.2)	0.91 (0.26)	0.91
	Single 0.5-g i.v. bolus; 3 (0%) (Foord, 1976)	NA	9.92	11.6 (3.4)	1.17	50.4 (6)	47.2 (15)	0.94	1.1 (0.1)	0.91 (0.26)	0.83
	Single 1-g i.v. bolus; 3 (0%) (Foord, 1976)	NA	11.01	11.6 (3.4)	1.05	90.8 (7.9)	94.4 (30.3)	1.04	1.1 (0.3)	0.91 (0.26)	0.83
	Single 1.5-g i.v. infusion; 23 (22%) (Kagedal et al., 2007)	NA	12.10	11.2 (3.3)	0.93	124	145 (44)	1.17	1.3	0.91 (0.25)	0.70
	Single 0.75-g i.v. bolus; 3 (0%) (O'Callaghan and Harding, 1977)	NA	9.52	11.1 (3)	1.17	78.8	72.5 (19.4)	0.92	1.267	0.90 (0.23)	0.71
	Single 1.5-g i.v. bolus; 3 (0%) (O'Callaghan and Harding, 1977)	NA	8.67	11.1 (3)	1.28	173	145 (39)	0.84	1.2	0.90 (0.23)	0.75
	Single 0.75-g i.v. bolus; 10 (100%) (Philipson and Stiernstedt, 1982)	NA	11.9 (1.6)	11.0 (2.8)	0.92	60.8 (8.6)	75.0 (19)	1.23	0.97 (0.13)	0.80 (0.18)	0.82
	Single 0.75-g i.m.; 6 (100%) (Harding et al., 1979)	NA	9.44	10.1 (2.7)	1.07	78.0	77.4 (20)	0.99	1.0	0.88 (0.17)	0.88
	Single 0.75-g i.m.; 6 (0%) (Foord, 1976)	NA	8.43	11.8 (3.6)	1.40	88.6	69.9 (23.3)	0.79	NA	0.95 (0.25)	NA
	Single 1-g i.m.; 5 (0%) (Foord, 1976)	NA	9.87	11.9 (3.7)	1.20	101.3	92.3(31)	0.91	NA	0.93 (0.25)	NA

TABLE 1 *continued*

	Study design; Population *n* (%F)	GWs	CL (l/h)			AUC (mg h/l)			Half-Life (h)		
			Obs	Pred	Ratio	Obs	Pred	Ratio	Obs	Pred	Ratio
	Single 0.75-g i.m.; 12 (0%) (O'Callaghan and Harding, 1977)	NA	NA	11.9 (3.8)	NA	68.0	69.5 (22)	1.02	1.0	1.0 (0.24)	1.00
	Single 1-g i.m.; 8 (0%) (O'Callaghan and Harding, 1977)	NA	NA	11.9 (3.8)	NA	68.0	69.5 (22)	1.02	1.0	1.0 (0.24)	1.00
	Single 1.5-g i.m.; 4 (0%) (O'Callaghan and Harding, 1977)	NA	NA	12 (3.6)	NA	115	137 (47)	1.18	1.0	0.96 (0.24)	0.96
Pregnant	Single 0.75-g i.v. bolus; 7 (100%) (Philipson and Stiernstedt, 1982)	11–35	16.9 (2.0)	13.1 (3.7)	0.78	42.0 (5.2)	61.4 (16.4)	1.46	0.73 (0.10)	0.88 (0.30)	1.21
	Single 0.75-g i.v. bolus; 7 (100%) (Philipson and Stiernstedt, 1982)	40	15.5 (2.1)	12.9 (3.0)	0.83	46.7 (8.4)	61.3 (14.4)	1.31	0.87 (0.17)	1.45	1.67
	Single 1.5-g i.v. bolus; 13 (100%) (Holt et al., 1994)	38–40	NA	12.8 (3.0)	NA	NA	123 (28)	NA	NA	1.4 (0.2)	NA
	Single 0.750-g i.m.; 22 (100%) (Craft et al., 1981)	37–40	NA	13.7 (3.5)	NA	NA	58.3 (14)	NA	*1.4 (1.1–1.9)	*2.0 (1.2–5)	1.43

AUC, area under the concentration curve; CL, total systemic clearance; %F, percentage female.

Trial Design P3. Single intravenous dose of 500 mg cefazolin infused over 2 minutes (Philipson et al., 1987); 20 trials of six pregnant women at 19–33 GWs and aged 22–57 years.

Trial Design P4. Single intravenous bolus dose of 2000 mg cefazolin (Brown et al., 1990); 20 trials of 10 pregnant women at 23–32 GWs and aged 18–45 years.

Trial Design P5. Single intravenous dose of 2000 mg cefazolin infused over 30 minutes (Allegaert et al., 2009); 20 trials of 49 pregnant women at 17–40 GWs and aged 18–45 years.

Trial Design P6. Single intravenous bolus dose of 1000 mg cefazolin (Elkomy et al., 2014); 20 trials of 10 pregnant women at 39 GWs and aged 23–43 years.

Trial Design P7. Single intravenous bolus dose of 1000 mg cefazolin (Fiore Mitchell et al., 2001); 20 trials of 26 pregnant women at 37–40 GWs and aged 22–40 years.

Trial Design P8. Single intravenous dose of 2000 mg cefazolin infused over 7 minutes (Grupper et al., 2017); 20 trials of 32 pregnant women at 39 GWs and aged 25–37 years.

Trial Design P9. Single intravenous bolus dose of either 2000 or 3000 mg cefazolin (Kram et al., 2017); 20 trials of 65 pregnant women at 39 GWs and aged 27–32 years; concentration reported at 1.833 hours after dose administration.

Trial Design P10. Single intramuscular dose of 14 mg/kg mg cefazolin (Bernard et al., 1977); 20 trials of 40 pregnant women at 15–20 GWs and aged 18–45 years.

Amoxicillin

Amoxicillin is semisynthetic penicillin-derivative antibiotic with a broad spectrum of activity for treatment of several infections. It has a better absorption profile compared with cefuroxime and cefazolin and hence is available as oral preparations. It has been reported that amoxycillin absorption displays apparent saturation kinetics (Westphal et al., 1991). Amoxicillin is mainly eliminated through the kidney and where OAT3 has been reported to be a key component of the drug secretion and its activity changes during pregnancy (Peng et al., 2021).

Model Building

A PBPK compound model for amoxicillin was built using published physicochemical properties and experimental data as well as predictive algorithms within the Simulator (see Supplemental Table 1 for the list of the model input). Model building and verification results for nonpregnant subjects are also in the supplemental document. Amoxicillin undergoes hepatic biliary clearance (Maudgal et al., 1982), and this route of elimination was incorporated in the model (fitted using observed data; Dalhoff and Koeppe, 1982). The elimination through the kidney was also incorporated in the model using the MechKim model. The MechKim model was parametrized using permeability clearance on both sides of the renal cells and active transporters at the proximal tubules using the basolateral OAT3 uptake transporter (Peng et al., 2021). Amoxicillin renal OAT3 clearance was optimized using the reported observed data (Dalhoff and Koeppe, 1982). The model then extended to the oral route using a first-order absorption model. Parameter values for this model were fitted to recover observed plasma data after a 500 mg oral dose (Westphal et al., 1991). Predicted exposure in the nonpregnant and pregnant populations was compared with the observed data.

To extend the nonpregnant amoxicillin PBPK model to predict kinetics during pregnancy, the pregnancy population was used and the permeability-limited placenta model, together with the full PBPK fetal model, was selected. The fold change in the renal OAT3 transporter activity was included in the model as described in the cefazolin section. The obtained placental CL_{PD} clearance value of 0.0045 l/h/ml of placenta was calculated from amoxicillin HBD and PSA. The fetal amoxicillin CL_R was calculated from the adult amoxicillin CL_R, as described earlier under the cefuroxime example, resulted in a fetal amoxicillin CL_R estimate of 0.03985 l/h/kg fetal weight. The combined fetal CL_R + $CL_{intramembranous}$ (= 0.044 l/h/kg fetal weight) were incorporated in the model before executing the simulations. All other fetal tissue-to-plasma partition coefficients (Kps) were predicted within the Simulator using the Rodgers and Rowland method (Rodgers and Rowland, 2006) without any adjustment to the calculated tissue Kps.

TABLE 2

Predicted vs. observed maternal and fetal parameters ratios of cefuroxime, cefazolin, and amoxicillin in the umbilical cord
Predicted cord-maternal ratio was calculated based on the AUC for the predicted concentration profiles. Results are expressed as mean (range).

	Study design	GWs	Cord/Maternal		
			Obs	Pred*	Ratio
Cefuroxime	Single 0.75-g i.v. (n = 8) (Philipson and Stiernstedt, 1982)	40	1.1 ± 2.2 (0.3–6)[a]	0.83 (0.6–1.0)	0.8
	Multiple 1.5-g i.v. 3× daily (n = 15) (De Leeuw et al., 1993)	27–34	1.1[b]	0.84 (0.7–1.0)	0.8
	Single 0.75-g i.m. (n = 10 natural labor) (Craft et al., 1981)	37–40	0.83 (0.42–1.08)	0.82 (0.62–1.0)	1.01.6
	Single 0.75-g i.m. (n = 12 C-section) (Craft et al., 1981)	37–40	0.50 (0.18–0.75)	0.82 (0.62–1.0)	
	Single 0.75-g i.v. (n = 26) (Holt et al., 1994)	38–40	0.45	0.77 (0.6–1.0)	1.71.11.3
	Single 1.5-g i.v. (n = 18 in control group) (Lalic-Popovic et al., 2016)	40	0.71 ± 0.46	0.77 ± 0.10	
	Single 1.5-g i.v. (n = 21 in hypertensive group) (Lalic-Popovic et al., 2016)	40	0.59 ± 0.40	0.77 ± 0.10	
Cefazolin	Single 2-g i.v. (n = 7) (Brown et al., 1990)	23–32	0.19 (0.03–0.54)	0.15 (0.10–0.25)	0.80
	Single 1-g i.v. bolus (n = 20) (Elkomy et al., 2014)	36–40	0.41 (0.21–1.45)[c]	0.36 (0.23–0.61)[c]	0.88
	Single 2-g i.v.; (n = 65) (Kram et al., 2017)	38.9	0.47[d]	0.60 (0.28–1.56)[d]	1.3
	Single 3-g i.v.; (n = 19) (Kram et al., 2017)	38.5	0.62[d]	0.62 (0.29–.34)[d]	1.0
Amoxicillin	Single 1000-g i.v. (n = 35) (Zareba-Szczudlik et al., 2016)	37–40	1.3[e]	2.1 (1.1–5.3)[e] 0.91 (0.78–1.12)[f]	1.6[e]0.7
	Single 500-mg oral (n = 30) (Zareba-Szczudlik et al., 2017)	37–40	0.4	1.2 (0.8–1.2)[e] 0.93(0.75–1.06)[f]	3.02.3

[a]Geometric mean ± S.D. (range)
[b]Geometric mean for C_{8h}
[c]Median (range)
[d]Mean for $C_{1.8h}$
[e]Mean (range) for $C_{2.0h}$
[f]Mean (range) for AUC_{INF}

Predicted exposure in the pregnant populations was compared with the observed data. The following virtual trial designs were set for predicting amoxicillin in pregnant subjects after maternal administration:

Trial Design P1. Single 15-minute infusion of 1 g amoxicillin (Muller et al., 2008b); 20 trials of 34 pregnant women at 30–40 GWs and aged 20–38 years.

Trial Design P2. Single 30-minute infusion of 2 g amoxicillin (Muller et al., 2008b); 20 trials of 34 pregnant women at 30–40 GWs and aged 20–38 years.

Trial Design P3. A 30-minute infusion of 2 g amoxicillin followed by 15-minute infusion of 1 g amoxicillin (5 hours apart) (Muller et al., 2008a); 20 trials of 17 pregnant women at 30–37 GWs and aged 20–35 years.

Trial Design P4. Single oral dose of 500 mg amoxicillin (Andrew et al., 2007); 20 trials of 16 pregnant women at 18–22 GWs and aged 20–37 years.

Trial Design P5. Single oral dose of 500 mg amoxicillin (Andrew et al., 2007); 20 trials of 16 pregnant women at 30–34 GWs and aged 20–37 years.

Trial Design P6. Single intravenous bolus of 1000 mg amoxicillin (Zareba-Szczudlik et al., 2016); 20 trials of 35 pregnant women at 38 GWs and aged 20–40 years.

Trial Design P7. Single oral dose of 500 mg amoxicillin (Zareba-Szczudlik et al., 2017); 20 trials of 30 pregnant women at 38 GWs and aged 22–42 years.

Results

Cefuroxime. PBPK predictions for cefuroxime in plasma of nonpregnant subjects after intravenous and intramuscular administration are shown in Supplemental Fig. 1. Predicted cefuroxime exposure during pregnancy is given in Fig. 2A for maternal systemic exposure, umbilical cord plasma level, and amniotic fluid. Pregnancy and fetal concentration predictions were obtained using a fully bottom-up approach (i.e., without any parameter adjustment or fittings). Predicted exposure in different fetal organs is given in Fig. 2B. These results show adequate prediction of observed cefuroxime concentration profiles in nonpregnant and pregnant subjects as well as in the fetal organs. Comparison of the predicted PK parameters in nonpregnant subjects and during pregnancy for the simulated trials with those available from clinical studies is given in Table 1. The differences between simulated and observed PK parameters were within 2-fold. Comparison of the predicted umbilical-to-maternal ratio of cefuroxime obtained from the simulated trials with those available from clinical studies is given in Table 2.

Cefazolin. Predicted systemic concentration profiles of cefazolin in plasma as well as derived PK parameters were generally in agreement with the observed data. Cefazolin PBPK model predictions for plasma level in nonpregnant women after intravenous and intramuscular administration are given in Supplemental Fig. 2. Predicted cefazolin concentration-time profiles in pregnancy compared with the clinical data are shown in Fig. 3A for maternal systemic exposure, umbilical vein, and amniotic fluid and in Fig. 3B for different fetal organs. These results were obtained via the bottom-up approach for the fetoplacental model without any parameter adjustment and agree with the observed data. The observed data are within the predicted 5th–95th percentile range. Comparison of the predicted maternal cefazolin PK parameters obtained from the simulated trials with those available from clinical studies is given in Table 3. Comparison of the predicted cefazolin PK parameters obtained from the simulated trials with those available from clinical studies for the umbilical cord is given in Table 2.

Amoxicillin. PBPK predictions for amoxycillin in plasma of nonpregnant subjects after intravenous and oral administration with overlayed data from 20 clinical studies are shown in Supplemental Fig. 3. Comparison of the predicted versus observed amoxicillin PK parameters in nonpregnant subjects is shown in Table 4. These results show adequate model performance in the nonpregnant population. Predicted amoxicillin exposure during pregnancy is given in Fig. 4 for maternal systemic exposure, umbilical cord plasma level, and amniotic fluid. Predictions were obtained without any parameter adjustment and gave adequate prediction of observed amoxicillin concentration profiles during different trimesters as well as at term. Comparison of the predicted PK parameters during pregnancy for the simulated trials with those available from clinical studies is given in Table 4. The differences between simulated and observed PK parameters were within 2-fold. Limited data are available on amoxicillin exposure in the umbilical cord. Comparison of the predicted umbilical-to-maternal ratio of amoxicillin obtained from the simulated trials with those available from clinical studies is given in Table 2.

Discussion

The current study utilizes the bottom-up population-based PBPK approach to assess the performance of a fetal-maternal PBPK model within the Simcyp Simulator to predict maternal and fetal exposure without any fitting or adjustment to the physiologic-related or

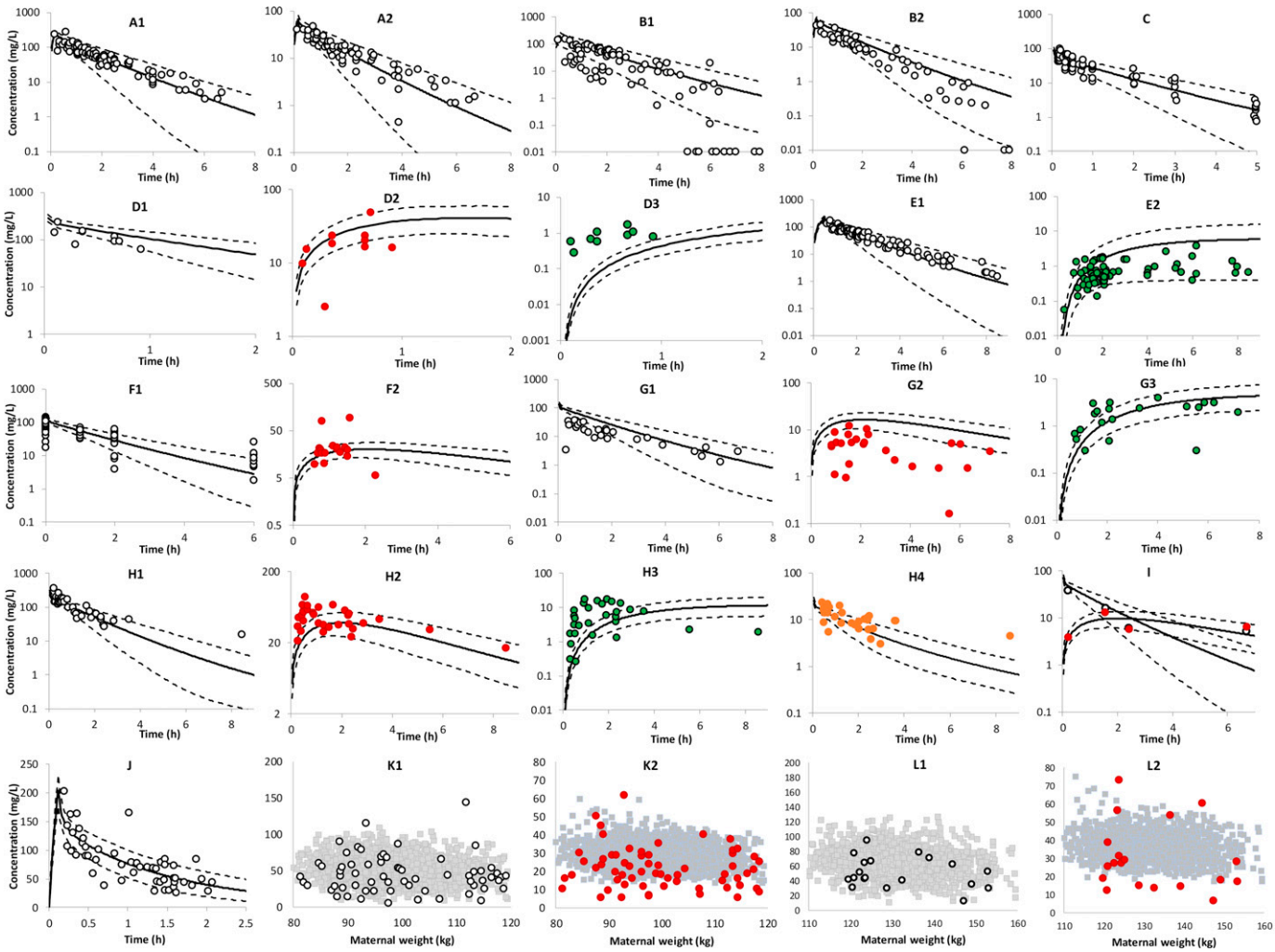

Fig. 3. (A) PBPK predicted vs. observed (circles) cefazolin concentration profiles in pregnant women after single intravenous doses. Plot A1 and A2: 17–28 GWs (van Hasselt et al., 2014); Plot B1 and B2: 28–40 GWs (van Hasselt et al., 2014); Plot C: 19–33 GWs (Bernard et al., 1977); Plot D: 23–32 GWs (Brown et al., 1990); Plot E: 17–40 GWs (Allegaert et al., 2009); Plot F: 39 GWs (Elkomy et al., 2014); Plot G: 37–40 GWs (Fiore Mitchell et al., 2001); and Plot H: 39 GWs (Grupper et al., 2017). Plots I and J are for predicted (diamonds) vs. observed cefazolin concentrations at 1.83 hours in maternal and umbilical at 39 GWs in overweight and obese pregnant women (Kram et al., 2017). Observed concentrations are shown as open circles (maternal), red circles (umbilical vein plasma), green circles (amniotic fluid), and orange circles (placental tissue). Bold continuous lines are the predicted means, and the broken lines are the 5th and 95th percentiles. See *Materials and Methods* for trial settings. (B) PBPK predicted vs. observed (circles) maternal, placental, amniotic, and fetal cefazolin concentration after administration of a single intramuscular dose of 14 mg/kg cefazolin (Bernard et al., 1977) to pregnant women at 15–20 GWs. Observed concentrations are shown as open circles (maternal), red circles (umbilical vein plasma), green circles (amniotic fluid), and orange circles (placental tissue). Bold continuous lines are the predicted means, and the broken lines are the 5th and 95th percentiles. See *Materials and Methods* for trial settings. Horizontal lines represent the least detectable values measured during the sampling window, as the exact sampling time was unknown; the horizontal solid line in the fetal brain plot represents the measured cerebrospinal fluid value.

compound-related parameters during pregnancy. Predicted parameters and profiles were compared against observed data taken from independent studies. The physiologically related PBPK model parameters that account for gestational age-dependent physiology in the mother and the fetus, together with the interindividual variability (Abduljalil et al., 2012; 2018; 2019; 2020a; 2021), were also incorporated within the model to facilitate the prediction of drug kinetics at different gestational weeks. The transplacental diffusions of these compounds were calculated using the physicochemical properties of the drug and integrated within the fetal-maternal PBPK model to determine fetal exposure.

The maternal renal clearance of cefuroxime and cefazolin was described using OAT3 and MRP4 transporters within the MechKiM model (Fig. 1). The maternal blood flow and GFR in this model are gestational age-dependent according to previously published data (Abduljalil et al., 2012). For cefuroxime, the appropriateness of OAT3 was demonstrated by the in vivo-observed 40% reduction on cefuroxime clearance by competitive inhibition with probenecid and the increase in cefuroxime area under the concentration curve of 27% by coadministration of the OAT substrate NX-059, whereas the contribution of MRP4 was estimated and its appropriateness was verified against the observed cumulative fraction of drug excreted unchanged in urine over 12 hours (fe_{12h}) (for more details, see Hsu et al., 2014). Likewise, for cefazolin, the appropriateness of OAT3 contribution was verified against the observed 59% (vs. 62% predicted) reduction in cefazolin clearance with probenecid (Brown et al., 1993). The predicted and observed profiles (Supplemental Fig. 2) of plot 11 for control and 12 with probenecid treatment are in good agreement. The appropriateness of MRP4 contribution was verified against the observed cumulative amount of cefazolin excreted unchanged in urine over 12 hours (see Supplemental Fig. 4). The predicted fe_{12h} without MRP4 was 0.47 ± 0.12, whereas the predicted fe_{12h} with MRP4 was 0.89 ± 0.046. The lattervalue is within 1.19-fold of the observed mean of 0.76 ± 0.21 (Rattie and Ravin, 1975)

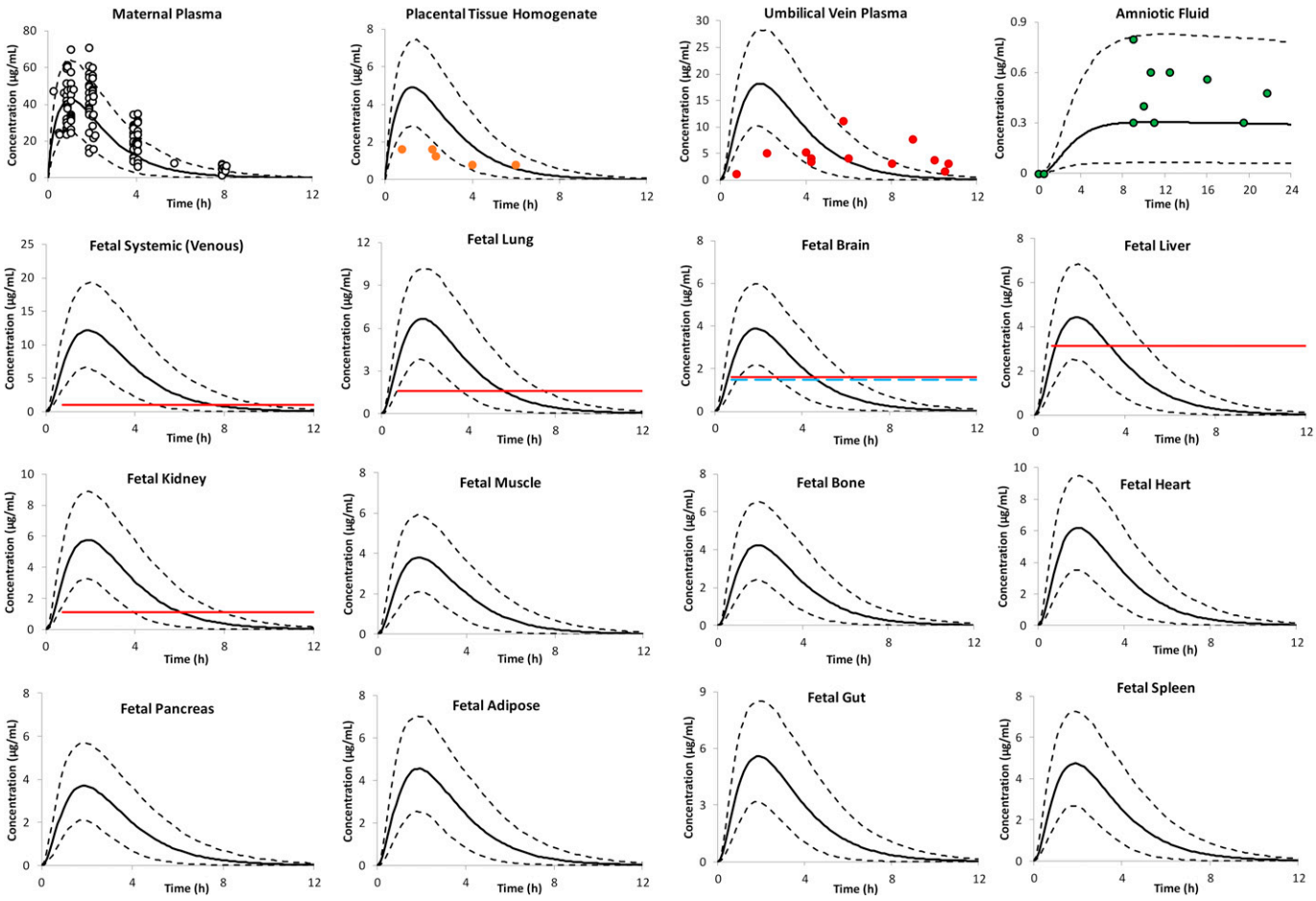

Fig. 3 (CONT.)

and 1.0-fold of the observed value of 0.89 ± 0.30 in single and multiple doses (Smyth et al., 1979).

Coupling the maternal cefuroxime PBPK model with the detailed fetoplacental compartments allowed prediction of cefuroxime disposition in the fetoplacental model (Fig. 2, A and B). Cefuroxime PK parameters during pregnancy have not been adequately reported and are limited to those shown in Tables 1 and 2. Cefuroxime clearance was reported to be 1.4 (predicted 1.2)- and 1.3 (predicted 1.2)-fold higher during pregnancy (11–35 GWs) and at delivery than in nonpregnant women in the same subjects ($n = 7$), respectively (Philipson and Stiernstedt, 1982). This increase in cefuroxime clearance can be partly explained by the increase in the glomerulus filtration or the increase in the activity of the involved OAT renal transporters. A recent work indicated that the activity of renal OAT1 at term is at nonpregnant capacity after being increased by 3-fold during the second trimester (Peng et al., 2021). It is still unclear at what rate this transporter operates during the first trimester. Although no informative data could be found to describe the changes in renal MRP4 transporter during pregnancy, the nonpregnant levels were assumed for these transporters to predict the drug kinetics during pregnancy in the current model. Since this cefuroxime PBPK model captured the pharmacokinetics in nonpregnant and pregnant populations adequately, including the observed increase in clearance during pregnancy, it seems that the impact of pregnancy on the activity of these transporters, at least for cefuroxime, is negligible (Fig. 2, A and B).

Calculated cefuroxime placental permeability using the physicochemical properties of the drug indicates rapid and significant permeation of the drug into the fetal circulation (i.e., $CL_{PD} = 1.06$ l/h). This clearance resulted in adequate predictions of the observed placental, umbilical cord, and fetal organ exposure (Takase et al., 1979; Bousfield et al., 1981; Craft et al., 1981; Philipson and Stiernstedt, 1982; Roumen et al., 1990; De Leeuw et al., 1993; Holt et al., 1993; 1994) (Fig. 2, B and C; Tables 1 and 2). Likewise, the calculated fetal renal, swallowing, and intramembranous clearances reflected the observed concentrations in the amniotic fluid (Fig. 2, A and B). The mean predicted cefuroxime cord-maternal plasma ratio was 0.8 (range: 0.6–1), which agrees with observed concentration ratio of 0.83 (0.42–1.08) sampled within 9.5 hours, 0.5 (0.18–0.75) sampled within 4.5 hours after drug administration (Craft et al., 1981), and 1.1 (0.3–6) sampled within the first 5 hours of drug administration (Philipson and Stiernstedt, 1982). Additional studies suggested a ratio of 1.5 (De Leeuw et al., 1993) and 0.45 (a mean of two groups of 0.6 and 0.3) (Holt et al., 1994).

The cefazolin PBPK predictions show good agreement with the observed data in nonpregnant and pregnant subjects. The developed model predicts an increasing cefazolin maternal clearance during pregnancy. The predicted systemic clearance increases by 70% of nonpregnant value at 20 GWs and gradually decreases to approximately 60% at term, which agrees with observed increases of 57% (Philipson et al., 1987) and 74% (Elkomy et al., 2014) in cefazolin clearance during pregnancy compared with postpartum values. The activity of renal OAT3 during pregnancy was incorporated as a continuous function to allow scaling the activity of this transporter at each gestational week. Calculated cefazolin placental permeability using the physicochemical properties of the drug resulted in a diffusion clearance of approximately

TABLE 3

Predicted vs. observed PK parameters of cefazolin in nonpregnant subjects and during pregnancy

Values are given as mean (S.D.). Simulated population size for each study was 20× actual study size.

			CL (l/h)			AUC (mg h/l)			Half-life (h)		
	Study design	**GWs**	**Obs**	**Pred**	**Ratio**	**Obs**	**Pred**	**Ratio**	**Obs**	**Pred**	**Ratio**
Nonpregnant	Single 2-g i.v.; 7M (Smyth et al., 1979)	NA	3.58	4.16 (1.32)	1.16	559 (93)	524 (149)	0.94	2.0 (0.3)	1.5(0.4)	0.75
	Single 3-g i.v.; 7M (Smyth et al., 1979)	NA	4.42	4.16 (1.32)	0.94	679 (123)	786 (223)	1.16	2.0 (0.2)	1.5 (0.4)	0.75
	Single 4-g i.v.; 7M (Smyth et al., 1979)	NA	4.56	4.16 (1.32)	0.91	878 (146)	1049 (297)	1.19	1.9 (0.2)	1.9 (0.47)	1.00
	Multiple 4-g 2× on day 5; 7M (Smyth et al., 1979)	NA	5.1	4.81 (1.3)	0.94	778 (88)	1041 (291)	1.34	1.8 (0.2)	1.9 (0.47)	1.05
	Multiple 4-g 2× on day 10; 7M (Smyth et al., 1979)	NA	4.94	4.81 (1.3)	0.97	810 (112)	1041 (291)	1.28	1.8 (0.2)	1.9 (0.47)	1.06
	Single 1-g (2-min inf); 17M (Rattie and Ravin, 1975)	NA	3.8	4.27 (1.43)	1.12	264	258 (78)	0.98	1.4	1.5 (0.4)	1.07
	Single 2-g (10-min inf); 6M (Brown et al., 1993)	NA	4.96	4.16 (1.33) < 2.48 (0.56)[a]>	0.84 <0.93[a]>	NA	525 (151) < 846 (175)[a]>	NA	1.6 <2.7[a]>	1.5 (0.38) < 1.9 (0.47)[a]>	1.00 < 0.7[a]>
			<2.68[a]>								
	Single 0.5-g (2-min inf); 6F (Philipson et al., 1987)	0	4.66 (0.74)	4.3 (1.2)	0.92	110 (21)	127 (33)	1.15	1.7 (0.3)	1.2 (0.4)	0.71
	Single 1-g bolus; 20F (Elkomy et al., 2014)	0	4.12	4.2 (1.3)	1.02	NA	257.4	NA	NA	1.2 (0.3)	NA
	Single 1-g i.m.; 11M (Scheld et al., 1981)	NA	NA	5.1 (2.1)	NA	218 (40)	227 (81)	1.04	2.1 (0.5)	1.5 (0.4)	0.72
	Single 1-g i.m.; 11M (Kirby and Regamey, 1973)	NA	NA	5.0 (2.1)	NA	NA	229 (83)	NA	1.8	1.5 (0.4)	0.84
Pregnant	Single 0.5-g i.v.; 6F (Philipson et al., 1987)	19–33	7.3 (3.0)	6.9 (2.6)	0.95	75.7 (27.6)	80.8 (24)	1.1	1.1 (0.1)	1.0 (0.3)	0.91
	Single 2-g (30-min inf); 49F (Allegaert et al., 2009)	17–40	7.44 (1.34)	7.03 (2.22)	0.94	269[b]	309 (87)	1.15	0.74[b]	1.25 (0.37)	1.69
	Single 2-g i.v.; 120F (van Hasselt et al., 2014)	17–27	7.48[b]	6.94 (2.7)	0.93	NA	322 (101)	NA	NA	1.3 (0.24)	NA
	Single 1-g or 2-g; 30F (van Hasselt et al., 2014)	28–40	7.54[b]	6.8 (2.3)	0.90	NA	266 (107)	NA	NA	1.3 (0.25)	NA
	Single 1-g bolus; 20F (Elkomy et al., 2014)	36–40	7.18 (0.56)	6.3 (1.8)	0.90	NA	170 (44)	NA	NA	1.2 (0.2)	NA
	Single 2-g (7-min inf); 32F (Grupper et al., 2017)	39	7.38 (5.34)	9.25 (2.58)	1.25	271	232 (60)	0.86	NA	1.1 (0.3)	NA

AUC, area under the concentration curve; CL, systemic clearance; F, female; inf, infusion; M, male.

[a]Values in the presence of probenecid.

[b]Values were calculated using the reported PK parameter means.

TABLE 4

Predicted vs. observed PK parameters of amoxicillin in nonpregnant subjects and during pregnancy after intravenous or oral administration
Results are expressed as mean (S.D.); *mean (range).

			CL (l/h)			AUC (mg h/l)			Half-life (h)		
	Study Design; Population n (%F)	GWs	Obs	Pred	Ratio	Obs	Pred	Ratio	Obs	Pred	Ratio
Nonpregnant	0.25-g i.v. bolus; 7 (0%) (Dalhoff and Koeppe, 1982)	NA	12.2	14.8 (3.7)	1.30	20.57 (3.64)	18.1 (4.9)	0.88	NA	1.29 (0.47)	NA
	0.5-g i.v. infusion; 7 (0%) (Dalhoff and Koeppe, 1982)	NA	11.7	14.8 (3.7)	1.34	42.56 (6.4)	36.19 (9.83)	0.85	NA	1.29 (0.47)	NA
	1-g i.v. bolus; 7 (0%) (Dalhoff and Koeppe, 1982)	NA	12.4	14.8 (3.7)	1.19	80.57 (9.75)	72.4 (19.7)	0.90	NA	1.29 (0.47)	NA
	0.25-g i.v. bolus; 7 (0%) (Hill et al., 1980)	NA	15.2	14.8 (3.7)	0.97	16.5 (1.3)	18.1 (4.9)	1.10	1.19 (0.03)	1.29 (0.47)	1.08
	0.5-g i.v. bolus; 7 (0%) (Hill et al., 1980)	NA	16.0	14.8 (3.7)	0.93	31.3 (1.7)	36.2 (9.8)	1.16	1.25 (0.02)	1.29 (0.47)	1.03
	1-g i.v. bolus; 7 (0%) (Hill et al., 1980)	NA	15.5	14.8 (3.7)	0.95	64.6 (4.7)	72.4 (19.7)	1.12	1.11 (0.02)	1.29 (0.47)	1.16
	2-g i.v. 28-min inf; 7 (0%) (Hill et al., 1980)	NA	15.4	15.1 (3.9)	0.98	130 (10.7)	142 (39)	1.09	1.19 (0.05)	1.19 (0.32)	1.00
	5-g i.v. 28-min inf; 7 (0%) (Hill et al., 1980)	NA	12.9	15.1 (3.9)	1.17	386.3 (32.2)	354 (98)	0.92	1.32 (0.04)	1.19 (0.32)	0.90
	0.5-g i.v. bolus; 9 (22%) (Arancibia et al., 1980)	NA	13.5 (3.5)	15.8 (2.6)	1.17	37.0 (9.7)	36.6 (7.1)	0.86	1.08 (0.28)	0.83 (0.16)	0.74
	4-g i.v. 5-min inf; 12 (50%) (Adam et al., 1983)	NA	9.46 (1.4)	14.9 (3.8)	1.57	423 (62)	286.4 (75.5)	0.68	1.11 (2.2)	1.54 (0.8)	1.39
	1-g oral; 12 (50%) (Prevot et al., 1997)	NA	NA	29.9 (12.2)	NA	47.6 (12)	38.7 (14.8)	0.81	1.3 (0.2)	1.35 (0.38)	1.04
	1-g oral; 8 (0%) (Westphal et al., 1991)	NA	33.7	31.3 (12.0)	0.93	29.72 (5.3)	36.4 (13.3)	1.22	NA	1.42 (0.4)	NA
	0.25-g oral; 8 (0%) (Zarowny et al., 1974)	NA	27.3	31.3 (12.0)	1.15	9.17 (1.70)	9.45 (3.46)	1.03	1.05 (0.30)	1.42 (0.4)	1.35
	0.5-g oral; 12 (50%) (Pires de Abreu et al., 2003)	NA	21.0	27.8	1.32	23.8	18	0.76	1.2	1.33	1.11
	0.5-g oral; 12 (50%) (Adam et al., 1983)	NA	25.8	31.3 (12.3)	1.21	19.4 (4.5)	19.1 (7.3)	0.98	0.88 (0.18)	1.37 (0.39)	1.56
	0.5-g oral; 16 (100%) (Andrew et al., 2007)	NA	28.8 (16)	28.1 (11.1)	0.98	20.4 (6.6)	20.4 (7.5)	1.00	1.6 (0.2)	1.32 (0.37)	0.83
Pregnant	1-g 15-min inf; 34 (Muller et al., 2008b) (100%) (Philipson and Stiernstedt, 1982)	30–40	21.1 (19.6–23)	19.23 (12.3–28.2)	0.91	47.4	55.4	1.17	1.2 (0.2)	1.3 (0.3)	1.08
	2-g 30-min inf; 34 (Muller et al., 2008b)	30–40	21.1 (19.6–23)	19.23 (12.3–28.2)	0.91	94.8	111	1.17	1.2 (0.2)	1.3 (0.3)	1.08
	1-g inf, then 2-g inf (Muller et al., 2008a)	29–37	22.8	19.5 (5.0)	0.86	NA	NA	NA	1.1	0.92 (0.2)	0.84
	0.5-g oral; 16 (100%) (Andrew et al., 2007)	18–22	35.5 (8.5)	35.1 (14.1)	0.99	15.2 (5.6)	16.3 (6.0)	1.07	1.2 (0.5)	1.32 (0.36)	1.1
	0.5-g oral; 16 (100%) (Andrew et al., 2007)	30–34	34.5 (5.9)	35.3 (13.6)	1.02	14.9 (2.8)	16.1 (5.7)	1.08	1.3 (0.2)	1.42 (0.3)	1.1

AUC, area under the concentration curve; CL, total systemic clearance; %F, percentage female; inf, infusion.

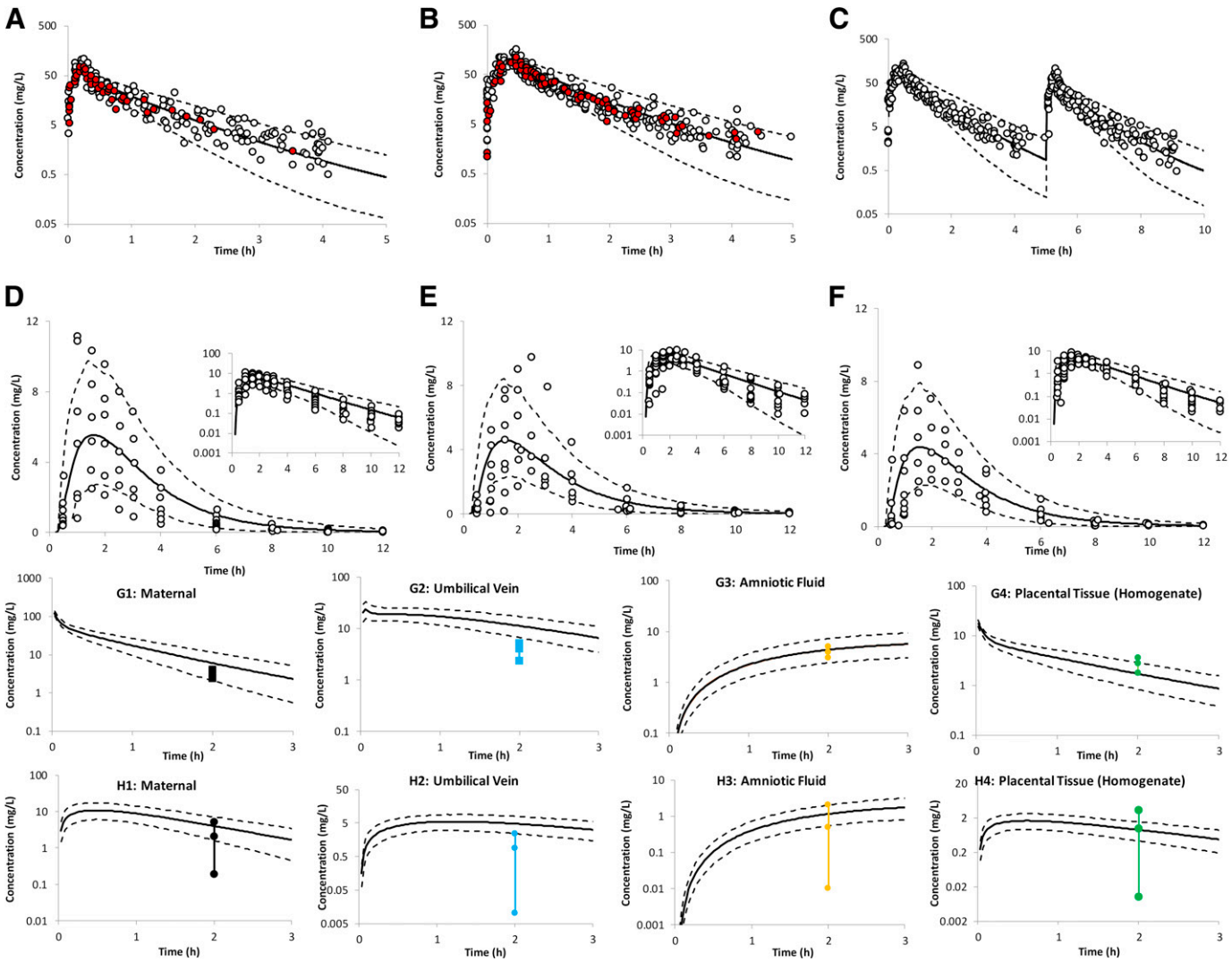

Fig. 4. PBPK predicted vs. observed (circles) amoxicillin concentration profiles in pregnant women after intravenous and oral administrations. Predictions after predelivery infusion doses of 1 g (Plot A; Muller et al., 2008b) and 2 g (Plot B; Muller et al., 2008b) amoxycillin (red circles = at labor, open circles = prelabor) and two consequent infusions of 2 g and 1 g amoxicillin prelabor (Plot C; Muller et al., 2008a). Oral doses of 500 mg in nonpregnant subjects (Plot D; Andrew et al., 2007), during second trimester (Plot E; Andrew et al., 2007), and during third trimester (Plot F; Andrew et al., 2007). Reported minimum, mean, and maximum measured amoxicillin concentration in different fetomaternal tissues after maternal amoxicillin administration of 1000 mg intravenously (Plot G1–G4; Zareba-Szczudlik et al., 2016) and orally (Plot H1–H4; Zareba-Szczudlik et al., 2017) at term. Bold continuous lines are the predicted means, and the broken lines are the 5th and 95th percentiles. See *Materials and Methods* for trial settings.

1 l/h, which indicates rapid and significant permeation of the drug into the fetal circulation. The predicted umbilical exposure at delivery described the observed exposure adequately (Fig. 3A). The predicted umbilical vein exposure is about 50% of the maternal plasma.

The observed changes in amoxicillin exposure during different trimesters were well captured using the developed gestational age-dependent renal OAT3 function. This case supports the adequacy of fold change in the activity of this transporter when applied to describe the disposition of cefazolin during pregnancy. Based on the limited observed amoxicillin concentration at 2 hours (Zareba-Szczudlik et al., 2016; 2017), the model predicted maternal, placenta, and amniotic exposure adequately but overpredicted the umbilical concentration (Fig. 4). Based on these results, the usefulness of the used physicochemical properties (i.e., HBD and PSA) to predict the umbilical exposure is still inconclusive.

Ratios of the predicted cord-maternal ratio against observed ratios from different studies are shown in Table 2. The umbilical cord and amniotic fluid drug concentration profiles in general do not change in parallel to the drug profile in the maternal circulation, even if placental transporters are not involved, especially after single-dose administration. This can be very prominent after single intravenous dose where, shortly after administration, the maternal concentration is at its maximum level but the umbilical concentration is almost zero. Quantification of the cord-maternal or amniotic-maternal ratios at specific time points will result in time-dependent cord-maternal ratio and make it difficult to compare ratios from different studies using different time points. For example, if the reported cord and maternal cefazolin concentrations in Fiore et al. (2001) is used to calculate the cord-maternal ratio during the first hour after drug administration, a mean value of 0.2 is obtained, which is less than the ratio of 0.52–0.62 reported by other studies (Elkomy et al., 2014; Kram et al., 2017). If the ratio is calculated from reported concentrations between 1.5 and 7 hours, when the umbilical cord concentration rises, a mean value of 0.6 is obtained, which agrees with other clinical studies as well as with the predicted ratio. A very low ratio of 0.16 was reported from seven pregnancies (Brown et al., 1990), owing primarily to the short sampling times of less than 1 hour.

Large variability in the clinical data has been observed, especially for the amniotic exposure, even after administration of comparable doses. Due to the nature of the conducted clinical studies, many of them reported lumped statistical results for wide gestational age ranges that stretched over two trimesters (Philipson and Stiernstedt, 1982; Holt et al., 1993; Allegaert et al., 2009), limited in the sample size (Philipson and Stiernstedt, 1982; Brown et al., 1990) and/or lumped data were reported from pregnant women received different doses (Bousfield et al., 1981; van Hasselt et al., 2014). Finally, it should be pointed out that the placental permeability results in the current study are predicted using an equation that was built to predict permeability through intestinal membrane from HBD counts and PSA of the relatively small compounds (Yang et al., 2007). Therefore, it is unlikely to be predictive for larger molecules with more HBD counts or where specific placental transports are involved as in the case of vancomycin, amikacin, or gentamicin (Akour et al., 2015).

The obtained permeability from this function is in length/time unit, and the placental surface area was used to scale this value to volume/time/placenta to represent placental permeability clearance. Although the predicted transplacental diffusion was verified with available maternal, umbilical, amniotic, and placental data at term (Figs. 2A, 3A, and 4), the availability of cefuroxime (Takase et al., 1979) and cefazolin (Bernard et al., 1977) data from different fetal organs allowed us to challenge the implemented model to simultaneously assess the integrity of dynamic physiology and drug properties for predicting fetal cefuroxime exposure at term (Fig. 2B) as well as cefazolin exposure at the end of the first trimester (Fig. 3B) without any parameter adjustment. The obtained adequate predictions of umbilical and fetal organ exposure in both cases reinforces the utility of the proposed models. Since data on placental transporter kinetics are still not available for all compounds investigated in the current work, their transplacental passages were described assuming passive permeability.

The extramembranous drug flow into and from the amniotic fluid was set to zero in this study, as this clearance pathway and how it is affected by underlying disease conditions are poorly understood. This limitation may contribute to the underprediction of early amniotic exposure observed in a few studies.

Conclusion

The detailed maternal-fetal PBPK model developed in this work successfully predicted the drug kinetics of cefuroxime, cefazolin, and amoxicillin during pregnancy. The model provided insight into the exposure within different fetal organs supported by limited observations. This was facilitated by parametrizing the diffusion clearance through the blood-placenta barrier scaled up from physicochemical properties of the drugs without any refinement of the model parameters. There is a need for more work in this area to characterize the drug transfer from and into the amniotic fluid of those antibiotics. The development of a pregnancy PBPK model is a promising approach to predict not only maternal and umbilical but also fetal tissue exposure at different stages of pregnancy. This study demonstrates the utility of the pregnancy PBPK modeling as a generic tool for predicting maternal and fetal kinetics of renally excreted drugs and can be used for assessing dose adjustment. The fetal PBPK model should be viewed as a "live" model that undergoes continuous enhancements as knowledge of mechanisms of drug distribution and elimination within the fetoplacental unit increases. Although the level of confidence in these models at any given time reflects the state of existing knowledge and the capability to incorporate such knowledge, they can play an important role in understanding safety and efficacy of drugs for both the mother and the developing fetus. The developed PBPK models provides an important and promising approach in the optimal design of clinical PK studies to predict maternal and fetal drug exposure at different stages of pregnancy.

Acknowledgments

We thank Eleanor Savill and Anna Kenworthy for their assistance with collecting the references and preparing the manuscript.

Authorship Contributions

Participated in research design: Abduljalil.

Conducted experiments: Abduljalil, Ning, Pansari, Pan.

Performed data analysis: Abduljalil, Ning, Pansari, Pan.

Wrote or contributed to the writing of the manuscript: Abduljalil, Ning, Pansari, Pan, Jamei.

References

Abduljalil K and Badhan RKS (2020) Drug dosing during pregnancy-opportunities for physiologically based pharmacokinetic models. *J Pharmacokinet Pharmacodyn* **47**:319–340.

Abduljalil K, Furness P, Johnson TN, Rostami-Hodjegan A, and Soltani H (2012) Anatomical, physiological and metabolic changes with gestational age during normal pregnancy: a database for parameters required in physiologically based pharmacokinetic modelling. *Clin Pharmacokinet* **51**:365–396.

Abduljalil K, Jamei M, and Johnson TN (2019) Fetal physiologically based pharmacokinetic models: systems information on the growth and composition of fetal organs. *Clin Pharmacokinet* **58**:235–262.

Abduljalil K, Jamei M, and Johnson TN (2020a) Fetal physiologically based pharmacokinetic models: systems information on fetal blood components and binding proteins. *Clin Pharmacokinet* **59**:629–642.

Abduljalil K, Johnson TN, and Rostami-Hodjegan A (2018) Fetal physiologically-based pharmacokinetic models: systems information on fetal biometry and gross composition. *Clin Pharmacokinet* **57**:1149–1171.

Abduljalil K, Pan X, Clayton R, Johnson TN, and Jamei M (2021) Fetal physiologically based pharmacokinetic models: systems information on fetal cardiac output and its distribution to different organs during development. *Clin Pharmacokinet* **60**:741–757.

Abduljalil K, Pansari A, and Jamei M (2020c) Prediction of maternal pharmacokinetics using physiologically based pharmacokinetic models: assessing the impact of the longitudinal changes in the activity of CYP1A2, CYP2D6 and CYP3A4 enzymes during pregnancy. *J Pharmacokinet Pharmacodyn* **47**:361–383.

Adam D, Koeppe P, and Heilmann HD (1983) Pharmacokinetics of amoxicillin and flucloxacillin following the simultaneous intravenous administration of 4 g and 1 g, respectively. *Infection* **11**:150–154.

Akour AA, Kennedy MJ, and Gerk PM (2015) The role of megalin in the transport of gentamicin across BeWo cells, an in vitro model of the human placenta. *AAPS J* **17**:1193–1199.

Allegaert K, van Mieghem T, Verbesselt R, de Hoon J, Rayyan M, Devlieger R, Deprest J, and Anderson BJ (2009) Cefazolin pharmacokinetics in maternal plasma and amniotic fluid during pregnancy. *Am J Obstet Gynecol* **200**:170E1–170E7.

Alrammaal HH, Batchelor HK, Morris RK, and Chong HP (2019) Efficacy of perioperative cefuroxime as a prophylactic antibiotic in women requiring caesarean section: a systematic review. *Eur J Obstet Gynecol Reprod Biol* **242**:71–78.

Andrew MA, Easterling TR, Carr DB, Shen D, Buchanan ML, Rutherford T, Bennett R, Vicini P, and Hebert MF (2007) Amoxicillin pharmacokinetics in pregnant women: modeling and simulations of dosage strategies. *Clin Pharmacol Ther* **81**:547–556.

Arancibia A, Guttmann J, González G, and González C (1980) Absorption and disposition kinetics of amoxicillin in normal human subjects. *Antimicrob Agents Chemother* **17**:199–202.

Bernard B, Barton L, Abate M, and Ballard CA (1977) Maternal-fetal transfer of cefazolin in the first twenty weeks of pregnancy. *J Infect Dis* **136**:377–382.

Blackburn S (2007) *Maternal, fetal and neonatal physiology: a clinical perspective*, Saunders Elsevier, Philadelphia.

Bookstaver PB, Bland CM, Griffin B, Stover KR, Eiland LS, and McLaughlin M (2015) A review of antibiotic use in pregnancy. *Pharmacotherapy* **35**:1052–1062.

Bouazza N, Foissac F, Hirt D, Urien S, Benaboud S, Lui G, and Treluyer JM (2019) Methodological approaches to evaluate fetal drug exposure. *Curr Pharm Des* **25**:496–504.

Bousfield P, Browning AK, Mullinger BM, and Elstein M (1981) Cefuroxime: potential use in pregnant women at term. *Br J Obstet Gynaecol* **88**:146–149.

Boyd PA (1984) Quantitative structure of the normal human placenta from 10 weeks of gestation to term. *Early Hum Dev* **9**:297–307.

Brown CE, Christmas JT, and Bawdon RE (1990) Placental transfer of cefazolin and piperacillin in pregnancies remote from term complicated by Rh isoimmunization. *Am J Obstet Gynecol* **163**:938–943.

Brown G, Zemcov SJ, and Clarke AM (1993) Effect of probenecid on cefazolin serum concentrations. *J Antimicrob Chemother* **31**:1009–1011.

Ci L, Kusuhara H, Adachi M, Schuetz JD, Takeuchi K, and Sugiyama Y (2007) Involvement of MRP4 (ABCC4) in the luminal efflux of ceftizoxime and cefazolin in the kidney. *Mol Pharmacol* **71**:1591–1597.

Craft I, Mullinger BM, and Kennedy MR (1981) Placental transfer of cefuroxime. *Br J Obstet Gynaecol* **88**:141–145.

Dalhoff A and Koeppe P (1982) Comparative pharmacokinetic analysis of amoxycillin using open two and three-compartment models. *Eur J Clin Pharmacol* **22**:273–279.

De Leeuw JW, Roumen FJ, Bouckaert PX, Cremers HM, and Vree TB (1993) Achievement of therapeutic concentrations of cefuroxime in early preterm gestations with premature rupture of the membranes. *Obstet Gynecol* **81**:255–260.

De Sousa Mendes M, Lui G, Zheng Y, Pressiat C, Hirt D, Valade E, Bouazza N, Foissac F, Blanche S, Treluyer JM, et al. (2017) A physiologically-based pharmacokinetic model to predict

human fetal exposure for a drug metabolized by several CYP450 pathways. *Clin Pharmacokinet* **56**:537–550.
Elkomy MH, Sultan P, Drover DR, Epshtein E, Galinkin JL, and Carvalho B (2014) Pharmacokinetics of prophylactic cefazolin in parturients undergoing cesarean delivery. *Antimicrob Agents Chemother* **58**:3504–3513.
Fiore Mitchell T, Pearlman MD, Chapman RL, Bhatt-Mehta V, and Faix RG (2001) Maternal and transplacental pharmacokinetics of cefazolin. *Obstet Gynecol* **98**:1075–1079.
Foord RD (1976) Cefuroxime: human pharmacokinetics. *Antimicrob Agents Chemother* **9**:741–747.
Garton AM, Rennie RP, Gilpin J, Marrelli M, and Shafran SD (1997) Comparison of dose doubling with probenecid for sustaining serum cefuroxime levels. *J Antimicrob Chemother* **40**:903–906.
Gower PE and Dash CH (1977) The pharmacokinetics of cefuroxime after intravenous injection. *Eur J Clin Pharmacol* **12**:221–227.
Grupper M, Kuti JL, Swank ML, Maggio L, Hughes BL, and Nicolau DP (2017) Population pharmacokinetics of cefazolin in serum and adipose tissue from overweight and obese women undergoing Cesarean delivery. *J Clin Pharmacol* **57**:712–719.
Harding SM, Eilon LA, and Harris AM (1979) Factors affecting the intramuscular absorption of cefuroxime. *J Antimicrob Chemother* **5**:87–93.
Hill SA, Jones KH, and Lees LJ (1980) Pharmacokinetics of parenterally administered amoxycillin. *J Infect* **2**:320–332.
Holt DE, Broadbent M, Spencer JA, de Louvois J, Hurley R, and Harvey D (1994) The placental transfer of cefuroxime at parturition. *Eur J Obstet Gynecol Reprod Biol* **54**:177–180.
Holt DE, Fisk NM, Spencer JA, de Louvois J, Hurley R, and Harvey D (1993) Transplacental transfer of cefuroxime in uncomplicated pregnancies and those complicated by hydrops or changes in amniotic fluid volume. *Arch Dis Child* **68**:54–57.
Hsu V, de L T Vieira M, Zhao P, Zhang L, Zheng JH, Nordmark A, Berglund EG, Giacomini KM, and Huang SM (2014) Towards quantitation of the effects of renal impairment and probenecid inhibition on kidney uptake and efflux transporters, using physiologically based pharmacokinetic modelling and simulations. *Clin Pharmacokinet* **53**:283–293.
Hvidberg H, Struve C, Krogfelt KA, Christensen N, Rasmussen SN, and Frimodt-Møller N (2000) Development of a long-term ascending urinary tract infection mouse model for antibiotic treatment studies. *Antimicrob Agents Chemother* **44**:156–163.
Kågedal M, Nilsson D, Huledal G, Reinholdsson I, Cheng YF, Asenblad N, Pekar D, and Borgå O (2007) A study of organic acid transporter mediated pharmacokinetic interaction between NXY-059 and cefuroxime. *J Clin Pharmacol* **47**:1043–1048.
Kirby WM and Regamey C (1973) Pharmacokinetics of cefazolin compared with four other cephalosporins. *J Infect Dis* **128** (Suppl):S341–S346.
Kram JJF, Greer DM, Cabrera O, Burlage R, Forgie MM, and Siddiqui DS (2017) Does current cefazolin dosing achieve adequate tissue and blood concentrations in obese women undergoing cesarean section? *Eur J Obstet Gynecol Reprod Biol* **210**:334–341.
Lalic-Popovic M, Paunkovic J, Grujic Z, Golocorbin-Kon S, Milasinovic L, Al-Salami H, and Mikov M (2016) Decreased placental and transcellular permeation of cefuroxime in pregnant women with diabetes. *J Diabetes* **8**:238–245.
Lee SM, Park SK, Shim SS, Jun JK, Park JS, and Syn HC (2007) Measurement of fetal urine production by three-dimensional ultrasonography in normal pregnancy. *Ultrasound Obstet Gynecol* **30**:281–286.
Maged AM, Abdelmoneim A, Said W, and Mostafa WA (2014) Measuring the rate of fetal urine production using three-dimensional ultrasound during normal pregnancy and pregnancy-associated diabetes. *J Matern Fetal Neonatal Med* **27**:1790–1794.
Mathialagan S, Piotrowski MA, Tess DA, Feng B, Litchfield J, and Varma MV (2017) Quantitative prediction of human renal clearance and drug-drug interactions of organic anion transporter substrates using in vitro transport data: a relative activity factor approach. *Drug Metab Dispos* **45**:409–417.
Maudgal DP, Maxwell JD, Lees LJ, and Wild RN (1982) Biliary excretion of amoxycillin and ceftriaxone after intravenous administration in man. *Br J Clin Pharmacol* **14**:213–217.
Mayhew TM (2001) Fibrin-type fibrinoid in human placenta: a stereological analysis of its association with intervillous volume and villous surface area. *Image Anal Stereol* **20**:1–7.
Muanda FT, Sheehy O, and Bérard A (2017) Use of antibiotics during pregnancy and the risk of major congenital malformations: a population based cohort study. *Br J Clin Pharmacol* **83**:2557–2571.
Muller AE, DeJongh J, Oostvogel PM, Voskuyl RA, Dorr PJ, Danhof M, and Mouton JW (2008a) Amoxicillin pharmacokinetics in pregnant women with preterm premature rupture of the membranes. *Am J Obstet Gynecol* **198**:108E1–108E6.
Muller AE, Dörr PJ, Mouton JW, De Jongh J, Oostvogel PM, Steegers EA, Voskuyl RA, and Danhof M (2008b) The influence of labour on the pharmacokinetics of intravenously administered amoxicillin in pregnant women. *Br J Clin Pharmacol* **66**:866–874.
Neuhoff S, Gaohua L, Burt H, Jamei M, Li L, Tucker GT, and Rostami-Hodjegan A (2013) Accounting for transporters in renal clearance: towards a mechanistic kidney model (Mech KiM), in *Transporters in Drug Development* (Sugiyama Y and Steffansen B eds) in *AAPS Advances in the Pharmaceutical Sciences Series*, **vol 7**, pp 155–177, Springer, New York.
O'Callaghan CH and Harding SM (1977) The pharmacokinetics of cefuroxime in man in relation to its antibacterial activity. *Proc R Soc Med* **70** (Suppl 9):4–10.
Pacifici GM (2006) Placental transfer of antibiotics administered to the mother: a review. *Int J Clin Pharmacol Ther* **44**:57–63.
Peng J, Ladumor MK, and Unadkat JD (2021) Prediction of pregnancy-induced changes in secretory and total renal clearance of drugs transported by organic anion transporters. *Drug Metab Dispos* **49**:929–937.
Philipson A and Stiernstedt G (1982) Pharmacokinetics of cefuroxime in pregnancy. *Am J Obstet Gynecol* **142**:823–828.
Philipson A, Stiernstedt G, and Ehrnebo M (1987) Comparison of the pharmacokinetics of cephradine and cefazolin in pregnant and non-pregnant women. *Clin Pharmacokinet* **12**:136–144.
Pires de Abreu LR, Ortiz RM, de Castro SC, and Pedrazzoli Jr J (2003) HPLC determination of amoxicillin comparative bioavailability in healthy volunteers after a single dose administration. *J Pharm Pharm Sci* **6**:223–230.
Prevot MH, Jehl F, and Rouveix B (1997) Pharmacokinetics of a new oral formulation of amoxicillin. *Eur J Drug Metab Pharmacokinet* **22**:47–52.
Rattie ES and Ravin LJ (1975) Pharmacokinetic interpretation of blood levels and urinary excretion data for cefazolin and cephalothin after intravenous and intramuscular administration in humans. *Antimicrob Agents Chemother* **7**:606–613.
Rayburn WF and Farmer KC (1997) Off-label prescribing during pregnancy. *Obstet Gynecol Clin North Am* **24**:471–478.
Rhodin MM, Anderson BJ, Peters AM, Coulthard MG, Wilkins B, Cole M, Chatelut E, Grubb A, Veal GJ, Keir MJ, et al. (2009) Human renal function maturation: a quantitative description using weight and postmenstrual age. *Pediatr Nephrol* **24**:67–76.
Rodgers T and Rowland M (2006) Physiologically based pharmacokinetic modelling 2: predicting the tissue distribution of acids, very weak bases, neutrals and zwitterions. *J Pharm Sci* **95**:1238–1257.
Roumen FJ, Bouckaert PX, Cremers HM, and Vree TB (1990) Pharmacokinetics of cefuroxime in pregnant patients with preterm premature rupture of the membranes. *Pharm Weekbl Sci* **12**:275–279.
Schalkwijk S, Buaben AO, Freriksen JJM, Colbers AP, Burger DM, Greupink R, and Russel FGM (2018) Prediction of fetal darunavir exposure by integrating human ex-vivo placental transfer and physiologically based pharmacokinetic modeling. *Clin Pharmacokinet* **57**:705–716.
Scheld WM, Spyker DA, Donowitz GR, Bolton WK, and Sande MA (1981) Moxalactam and cefazolin: comparative pharmacokinetics in normal subjects. *Antimicrob Agents Chemother* **19**:613–619.
Schmidt A, Morales-Prieto DM, Pastuschek J, Fröhlich K, and Markert UR (2015) Only humans have human placentas: molecular differences between mice and humans. *J Reprod Immunol* **108**:65–71.
Smyth RD, Pfeffer M, Glick A, Van Harken DR, and Hottendorf GH (1979) Clinical pharmacokinetics and safety of high doses of ceforanide (BL-S786R) and cefazolin. *Antimicrob Agents Chemother* **16**:615–621.
Takase Z, Shirofuji H, and Uchida M (1979) Fundamental and clinical studies of cefuroxime in the field of obstetrics and gynecology. *Chemotherapy* **27** (Suppl. 6):600–602.
Teasdale F and Jean-Jacques G (1985) Morphometric evaluation of the microvillous surface enlargement factor in the human placenta from mid-gestation to term. *Placenta* **6**:375–381.
Thønnings S, Jensen KS, Nielsen NB, Skjønnemand M, Hansen DS, Lange KHW, and Frimodt-Møller N (2020) Cefuroxime pharmacokinetics and pharmacodynamics for intravenous dosage regimens with 750 mg or 1500 mg doses in healthy young volunteers. *J Med Microbiol* **69**:387–395.
Touboul C, Boulvain M, Picone O, Levaillant JM, Frydman R, and Senat MV (2008) Normal fetal urine production rate estimated with 3-dimensional ultrasonography using the rotational technique (virtual organ computer-aided analysis). *Am J Obstet Gynecol* **199**:57E1–57E5.
Underwood MA, Gilbert WM, and Sherman MP (2005) Amniotic fluid: not just fetal urine anymore. *J Perinatol* **25**:341–348.
van Dalen R, Vree TB, Hafkenscheid JC, and Gimbrère JS (1979) Determination of plasma and renal clearance of cefuroxime and its pharmacokinetics in renal insufficiency. *J Antimicrob Chemother* **5**:281–292.
van Hasselt JG, Allegaert K, van Calsteren K, Beijnen JH, Schellens JH, and Huitema AD (2014) Semiphysiological versus empirical modelling of the population pharmacokinetics of free and total cefazolin during pregnancy. *BioMed Res Int* **2014**:897216.
Verhagen CA, Mattie H, and Van Strijen E (1994) The renal clearance of cefuroxime and ceftazidime and the effect of probenecid on their tubular excretion. *Br J Clin Pharmacol* **37**:193–197.
Viel-Theriault I, Fell DB, Grynspan D, Redpath S, and Thampi N (2019) The transplacental passage of commonly used intrapartum antibiotics and its impact on the newborn management: a narrative review. *Early Hum Dev* **135**:6–10.
Westphal JF, Deslandes A, Brogard JM, and Carbon C (1991) Reappraisal of amoxycillin absorption kinetics. *J Antimicrob Chemother* **27**:647–654.
Yang J, Jamei M, Yeo KR, Tucker GT, and Rostami-Hodjegan A (2007) Prediction of intestinal first-pass drug metabolism. *Curr Drug Metab* **8**:676–684.
Zareba-Szczudlik J, Romejko-Wolniewicz E, Lewandowski Z, Rozanska H, Malinowska-Polubiec A, Dobrowolska-Redo A, Wilczynski J, and Czajkowski K (2016) Evaluation of the amoxicillin concentrations in amniotic fluid, placenta, umbilical cord blood and maternal serum two hours after intravenous administration. *Neuroendocrinol Lett* **37**:403–409.
Zareba-Szczudlik J, Romejko-Wolniewicz E, Lewandowski Z, Rozanska H, Malinowska-Polubiec A, Dobrowolska-Redo A, Wilczynski J, and Czajkowski K (2017) Evaluation of the amoxicillin concentrations in amniotic fluid, placenta, umbilical cord blood and maternal serum two hours after oral administration. *Neuroendocrinol Lett* **38**:502–508.
Zarowny D, Ogilvie R, Tamblyn D, MacLeod C, and Ruedy J (1974) Pharmacokinetics of amoxicillin. *Clin Pharmacol Ther* **16**:1045–1051.
Zhang Z, Imperial MZ, Patilea-Vrana GI, Wedagedera J, Gaohua L, and Unadkat JD (2017) Development of a novel maternal-fetal physiologically based pharmacokinetic model I: insights that determine fetal drug exposure through simulations and sensitivity analyses. *Drug Metab Dispos* **45**:920–938.
Zhang Z and Unadkat JD (2017) Development of a novel maternal-fetal physiologically based pharmacokinetic model II: verification of the model for passive placental permeability drugs. *Drug Metab Dispos* **45**:939–946.

Address correspondence to: Khaled Abduljalil, Certara UK Limited, Simcyp Division, Level 2-Acero, 1 Concourse Way, Sheffield, S1 2BJ, UK. E-mail: Khaled.Abduljalil@certara.com